

TELEVISION PICTURE TRANSMISSION AND OPTICAL  
SIGNAL PROCESSING

by

OTTO MEIER

Dipl. El.-Ing., Swiss Federal Institute of Technology, 1965

A THESIS SUBMITTED IN PARTIAL FULFILMENT OF THE  
REQUIREMENTS FOR THE DEGREE OF

MASTER OF APPLIED SCIENCE

in the Department of  
Electrical Engineering

We accept this thesis as conforming to the  
required standard

Research Supervisor

Members of Committee

Head of Department

Members of the Department  
of Electrical Engineering

THE UNIVERSITY OF BRITISH COLUMBIA

JULY, 1968

In presenting this thesis in partial fulfilment of the requirements for an advanced degree at the University of British Columbia, I agree that the Library shall make it freely available for reference and Study. I further agree that permission for extensive copying of this thesis for scholarly purposes may be granted by the Head of my Department or by his representatives. It is understood that copying or publication of this thesis for financial gain shall not be allowed without my written permission.

Department of Electrical Engineering

The University of British Columbia  
Vancouver 8, Canada

Date July 22, 1968

## ABSTRACT

Optical signal processing is introduced as a tool for investigations in the field of television compression research. An optical signal processing system is designed, which performs the Fourier transform of a picture signal  $F[B(x,y)]$  and its reconstruction  $F^{-1}\{F[B(x,y)]\}$ . Some basic optical filtering experiments are performed in the spatial frequency plane, and the optical analogue of the frequency sampling theorem is demonstrated.

The Fourier transforms of test pattern pictures show large gaps which can be used for compression. Observation of complex spectra of continuous tone pictures is found to be impaired by noise effects.

A physiological experiment is carried out, which investigates the relationship between tolerable flicker frequency and spatial frequency of a television picture. It is found that the tolerable flicker rate  $f_c$  decreases as the spatial frequency  $f_x$  is increased, according to the empirical equation  $f_c = f_0 \exp(-kf_x)$ .  $f_0$  and  $k$  are parameters depending on factors like contrast ratio, kind and size of picture, etc.

Compression systems using the above results are found to have a limit of obtainable compression ratio of approximately 3 to 1.

## TABLE OF CONTENTS

	Page
1. INTRODUCTION.....	1
2. THEORY OF OPTICAL SIGNAL PROCESSING.....	4
2.1 Fundamental optical systems.....	4
2.2 Optical filtering.....	8
3. DESIGN OF THE OPTICAL SYSTEM.....	11
3.1 Basic considerations.....	11
3.2 Calculations.....	13
3.3 The liquid cell.....	18
3.4 Frequency sampling arrangement.....	19
3.5 Description of the system.....	20
4. FOURIER TRANSFORMS AND SPATIAL FILTERING.....	24
4.1 Two-dimensional Fourier transforms.....	24
4.2 One-dimensional Fourier transforms.....	27
4.3 Relation to video signal.....	30
4.4 Frequency sampling.....	33
4.5 Coarse filtering.....	36
5. SPATIAL FREQUENCY FLICKER EXPERIMENTS.....	41
5.1 Basic idea.....	41
5.2 Test arrangement.....	42
5.3 Results.....	44
5.4 A tentative law.....	51
6. CONCLUSIONS AND FUTURE WORK.....	54
REFERENCES.....	57
APPENDIX.....	59

## LIST OF ILLUSTRATIONS

Figure		Page
1	Optical system for two-dimensional multiplication and integration.....	4
2	Optical Fourier transformer.....	6
3	Multichannel one-dimensional Fourier transformer..	7
4	Successive Fourier transformers.....	8
5	Variable scale Fourier transformer.....	12
6	Basic optical system.....	13
7	Diffraction grating.....	14
8	Liquid cell.....	19
9	Adjustable sampling grating.....	20
10	The final optical system.....	22
11	ROWI test chart.....	25
12	Two-dimensional Fourier transform of Figure 11....	25
13	Detail of ROWI test chart.....	26
14	Two-dimensional Fourier transform of Figure 13....	26
15	One-dimensional Fourier transform of ROWI test chart.....	28
16	Marconi resolution chart No. 1.....	29
17	One-dimensional Fourier transform of Marconi chart	29
18	One-dimensional Fourier transform of an aperture..	31
19	Part of the same transform as in Figure 18, only showing higher spatial frequencies.....	31
20	Fourier transform of aperture with empty transparency.....	32
21	Fourier transform of aperture with empty transparency in liquid cell.....	32
22	String of output pictures after frequency sampling	34
23	Single output picture without sampling.....	34

24	Central (zero order) output picture after frequency sampling .....	35
25	Enlarged part of sampled spatial frequency plane....	35
26	Output picture displayed on closed circuit television monitor .....	37
27	Effect of lowpass filter .....	38
28	Effect of highpass filter .....	38
29	Mask filter in Fourier transform plane of eq. 13....	38
30	Output from mask filter in Figure 29 .....	39
31	Fourier transform of a continuous tone picture ....	40
32	Sine wave response of the human eye .....	41
33	Flicker test arrangement .....	42
34	Optical flicker frequency as a function of spatial frequency for judgement "good" .....	45
35	Critical flicker frequency as a function of spatial frequency for judgement "acceptable" .....	46
36	Critical flicker frequency vs. contrast ratio .....	46
37	Critical flicker frequency with picture area as parameter .....	48
38	"Face" .....	49
39	"Group" .....	49
40	Critical flicker frequency of two half tone pictures	50
41	Bandlimited picture.....	50
42 & 43	View of test apparatus used for present work .....	53
A 1	Two-dimensional Fourier transformer .....	59
A 2	Geometrical relations .....	61

## ACKNOWLEDGEMENT

Many persons have helped in one or the other way during the course of this research project, and my thanks go to all of them.

In particular I would like to thank my supervisor, Dr. M. P. Beddoes, for many fruitful discussions and helpful suggestions, as well as for his invaluable assistance in preparing the thesis.

I would also like to thank Dr. A. D. Moore for reading and correcting the thesis.

Further thanks go to Mr. P. D. Carman and Mr. J. N. Cairns from NRC Ottawa, who provided the high quality lenses needed for this project.

I am grateful to Miss L. Ratcliffe and Mr. W. D. Ramsay for proofreading, and to Miss A. Hopkins for typing the thesis.

Finally, I would like to thank the administration of the University of British Columbia for my exchange Fellowship, and NRC for the financial support of this work.

## 1. INTRODUCTION

A considerable amount of work has been done in the field of image compression research, starting almost immediately after the invention of television. Numerous systems and techniques have been proposed to reduce the bandwidth required for the transmission of television signals, as becomes clear from Pratt's bibliography<sup>(1)</sup>. But, as Schreiber put it in a recent article: "The results are meager, indeed".<sup>(2)</sup> The work continues, because the need for a more efficient transmission system still exists. And, even though the practical results have been little, we at least begin to understand the problem.

Most of the present day work to reduce redundancy in television picture transmission is done on the basis of some digital techniques, investigating efficient coding and quantizing methods. Wide use of computer simulation is made to "realize" the coding methods, and only a very small part of the proposed systems have actually been built<sup>(1)</sup>.

In the last few years a new method of analysing and processing signals of various kinds has been developed, which makes use of coherent light, easily available today from lasers: Optical signal processing systems find increasing application in numerous fields of research and practical use.

Optical systems possess two degrees of freedom, i.e., two independent variables, as opposed to electronic systems with only one independent variable, time. In addition, optical systems show the property that a Fourier transform relation exists between the light amplitude distribution at the front- and back-focal planes of a lens used in the system. The optical system is capable of

performing Fourier transforms or related mathematical operations instantaneously in two dimensions; or, by use of astigmatic lenses, in one dimension with a number of independent channels. This makes it superior to an electronic system, which would have to use scanning or time sharing procedures to achieve the same results.

The very large number of points which can easily be processed in parallel fashion is another factor in favour of the optical method. A point against it is the noise, generated by the film material which carries the optical signal.

With optical methods, spatial frequency filtering is a simple operation in principle, and the research reported here uses such filtering as a tool to investigate some possibilities of bandwidth reduction for a picture signal.

There may be large gaps in the spectrum of a picture, which could be used for compression purposes, as suggested by vocoder methods in speech compression. An attempt was made to check on this point in Chapter 4.

Mertz and Gray first showed that the television spectrum is comb-like in structure, with empty spaces in between each clump of energy.<sup>(3)</sup> (This fact is made use of in carrier interlaced color television). Thus, we expect to be able to reduce bandwidth merely by closing up the spaces. In fact, the frequency version of the sampling theorem<sup>(4)</sup> suggests similar methods; a basic experiment described in this thesis shows that the spatial frequency spectrum of a still picture can be made infinitesimal in total, without affecting appreciably the picture quality.

For an active line of a normal television display, 300

spectral spikes have to be used in a frequency sampled signal, as will be shown in chapter 3.2. In principle, each line may be entirely uncorrelated, in which case the bandwidth needed for each spectral spike is roughly the number of picture lines times the picture repetition frequency:  $525 \times 30 = 15,750$  Hz, assuming single sideband modulation. Thus, although one single line of a still picture needs zero bandwidth, (in the limit), the television case needs  $300 \times 15,750$  Hz = 4.725 MHz; this happens to be the normal actual bandwidth.

Limitations in the perception of the human eye may be exploited to reduce television bandwidth. One such limitation is examined in this thesis. It is concerned with the question: What is the minimum rate at which the spatial frequencies must be presented on a TV-screen, for flicker to be just not apparent? It is shown that the minimum rate, or tolerable flicker frequency, decreases as the spatial frequency is increased.

Thus, a band reduced system could be designed, using different transmission rates for low and high frequency components of a television signal.

The present thesis deals with three problems:

- (a) The design of optical signal processing equipment, which can be used as a tool to investigate television compression problems (chapter 3);
- (b) The performance and results of some exploratory filtering experiments. These are not complete, but intended as a guide to further work (chapter 4);
- (c) The results of flicker experiments, which investigate the temporal response of the human eye to spatial frequencies (chapter 5).

## 2. THEORY OF OPTICAL SIGNAL PROCESSING

### 2.1 Fundamental optical systems

An excellent discussion of the theory of optical data processing is given by Cutrona et al.<sup>(5)</sup>. For the purpose of this thesis a brief description of the basic components and relations of an optical system is given here, discussing mainly the theory as it applies to investigations of the frequency domain.

Let us first consider an example of a non coherent light system, as it is shown in Fig. 1:

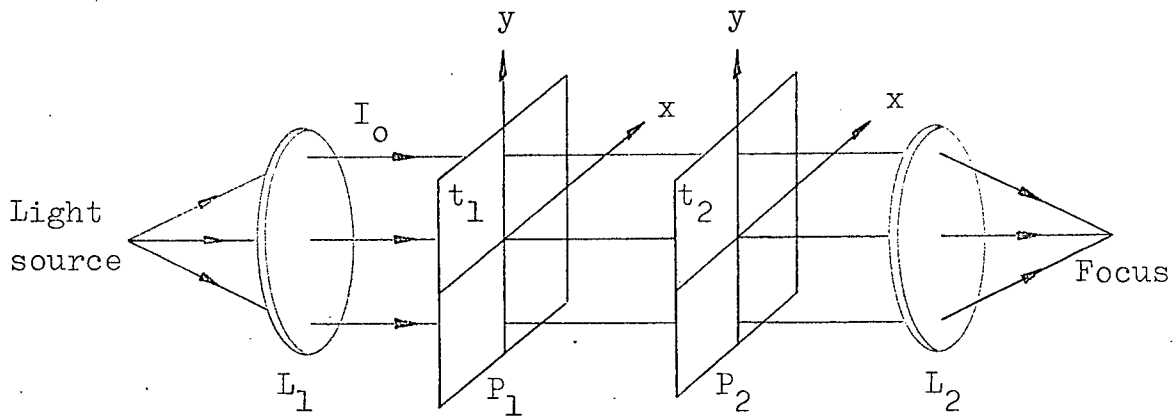


Fig. 1 Optical system for two dimensional multiplication and integration

A given signal of two variables may be represented by a spatially varying transparency, such as a photographic film, whose transmittance is  $t_1(x,y)$ , with  $0 \leq t_1 \leq 1$ . Light of uniform intensity  $I_0$  passes through this transparency and is spatially modulated to give the output intensity  $I_0 t_1(x,y)$ . If we now let this light pass through a second transparency of transmission  $t_2(x-X,y)$  for example, where  $X$  is a displacement of the transparency off the

axis of the light path, then the transmitted light will be of the intensity  $I_0 t_1(x,y)t_2(x-X,y)$ . Thus a two dimensional multiplication is performed.

Let a second lens  $L_2$  focus the light to a point, summing up all intensities to a total intensity  $I_p$ :

$$I_p = \iint_A I_0 t_1(x,y) t_2(x-X,y) dx dy \quad 2.1$$

$A$  is the total aperture area in plane  $P_1$ , and attenuation and effects of finite lens size have been ignored. (6)

This integral has the form of a two dimensional convolution or cross-correlation.

We defined the transmission function to be positive only. If we desire to represent a negative going signal, we must write it on a dc-bias, represented by a constant  $c$  in the transmission function. We may also have to introduce a scaling factor  $a$  for the original signal function.

$$t'_1 = c_1 + a_1 t_1(x,y) \quad 2.2$$

Evaluating an integral of the form of equation 2.1 will then produce undesired cross terms.

In many applications it is possible to remove the dc-bias by using a "coherent" optical system. Such a system requires the use of parallel, spatially coherent and monochromatic light. A Fourier transform of the transparency  $t'_1$  is obtained optically in this system, where the dc part of the signal is concentrated at one specific location. It may then be removed by a simple stop, and a second Fourier transform reconstructs the original signal



For a proof of equation 2.4 see appendix.

The spatial frequencies  $\omega_x$  and  $\omega_y$  are defined by relation 2.5:

$$\omega_x = \frac{-2\pi x_2}{\lambda F}, \quad \omega_y = \frac{-2\pi y_2}{\lambda F} \quad 2.5$$

where  $\lambda$  is the wavelength of the light used.

We see that  $\bar{U}_2$  is the Fourier transform of  $\bar{U}_1$ , lying within the limits  $\pm C$ ,  $\pm D$ . Plane  $P_2$  is the spatial frequency plane. The usefulness of a system according to Figure 2 can be seen immediately: Besides being a tool for spectrum analysis, filtering is easily accomplished by placing appropriate stops in the frequency plane to block any part of the spectrum.

To simulate and process the equivalent of a scanned signal, we need only a one-dimensional system. The second dimension can then be used to accommodate a large number of independent channels for one dimensional signals, thus not wasting the capacity of the system.

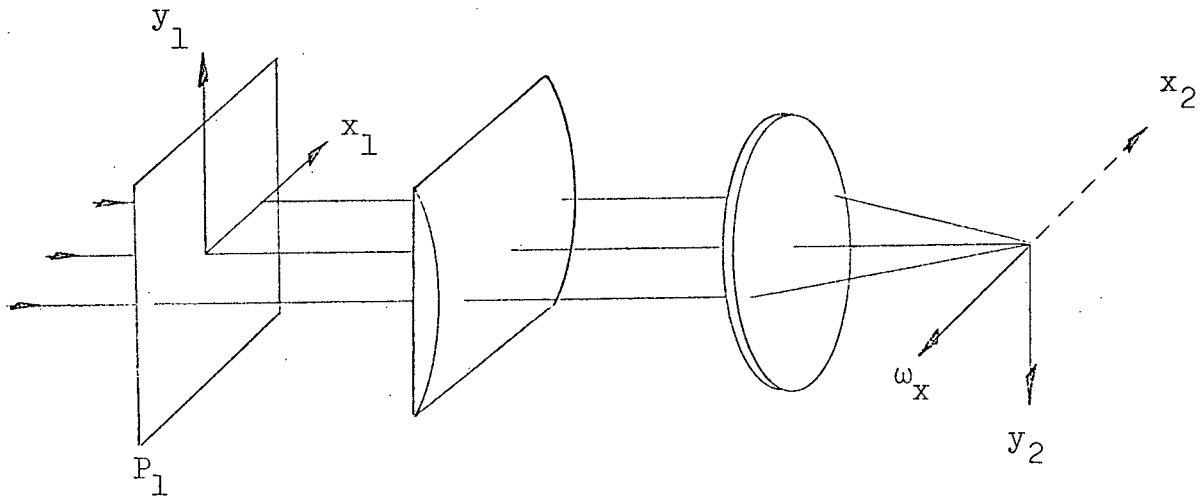


Fig. 3 Multichannel one-dimensional Fourier transformer

The lens system of Figure 3 focuses only in one dimension, performing an imaging in the other dimension, such that  $y_2$  is an inverted image of  $y_1$ . The Fourier transform obtained with this system therefore becomes

$$\bar{U}_2(x_2, y_2) = \int_{-C}^{+C} \bar{U}_1(x_1, y_1) \exp(-j\omega_x x_1) dx_1 \quad 2.6$$

Two or more Fourier transforming systems may be cascaded to perform successive transforms. The conventional Fourier transform theory requires the kernel function  $\exp(-j\omega t)$  for the transform from time to frequency domain, and the function  $\exp(j\omega t)$  for the inverse transform from frequency to time. An optical system (i.e., a lens) always introduces the kernel function  $\exp[-j(\omega_x x_1 + \omega_y y_1)]$ . We can obtain the right sign for the kernel function of the inverse transform by merely labelling the co-ordinates appropriately, as shown in Figure 4.

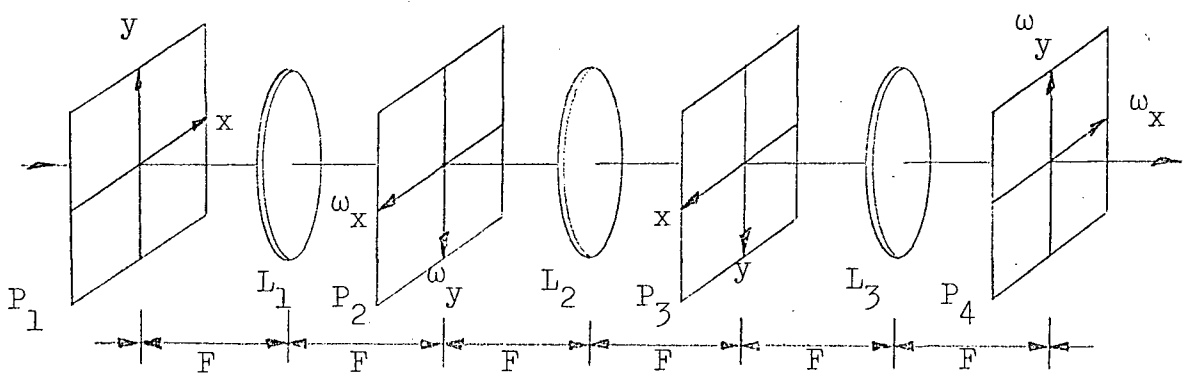


Fig. 4 Successive Fourier transformers

## 2.2 Optical filtering

It is possible to introduce filtering action on a signal

in the frequency plane of an optical system (plane  $P_2$ , Figure 4). The resulting effect can be observed immediately in the plane of the reconstruction ( $P_3$ , Figure 4). Basically there are two kinds of filters that may be introduced in the frequency plane: amplitude filters and phase filters. Together they can effect a complex filter function. An amplitude filter is obtained by varying the optical density of a transparency. A phase filter is realized by varying the thickness, which in turn varies the phase retardation. A simple form of an amplitude filter might be a slit, which corresponds to a spatial bandpass filter; a stop represents a rejection filter.

Complex filter functions appear to be possible, although more difficult to realize practically. A hologram, containing amplitude and phase information of a picture, can be used as a complex filter. Examples for this technique are to be found mainly in the field of pattern recognition<sup>(6)</sup>.

The one-dimensional Fourier transform plane may be sampled by narrow slits (infinitely narrow in the limit), spaced at regular intervals, to produce a perfect reconstruction. This is the optical analog of the frequency sampling theorem, which states that a time limited function can be represented by its uniform samples in the frequency domain.<sup>(4)</sup>

For each point in a line of a scanned picture, time has a distinct correspondence with each point in the x-direction in plane  $P_1$  of the optical system (Figure 3). The input signal will be a picture of finite size, placed into this plane, thus fulfilling the condition of a time limited signal. Now we can proceed to introduce some kind of a comb filter in the Fourier transform or spatial frequency plane  $P_2$ . The effect, observed at

the output plane  $P_3$  (see Figure 4), will be a diffraction due to the grating-like action of the comb filter, producing a string of diffracted output pictures. A coarse filter produces overlapping output images; the spacing of the grating lines has to be made fine enough (according to diffraction theory) in order to get the first maximum of the diffraction pattern at least one picture width off the optical axis (see chapter 3).

### 3. DESIGN OF THE OPTICAL SYSTEM

#### 3.1 Basic considerations

In the optical system described here Ronchi rulings were used as a comb filter to verify the frequency sampling theorem. These rulings are optically flat glass pieces with engraved, metal-filled lines of high precision, giving a 50/50 opaque/transpar-ent grating. They are readily available only with 500 lines per inch, which imposes some limits on the physical size of the whole system, because of the quite large diffraction length needed to get the diffracted output pictures separated in a one to one imaging system (see chapter 3.2.). One to one imaging was found to be desirable in order to allow easy observation of the output. A system using long focal length lenses is also better with respect to lens aberrations, because the "thin lens" concept is more closely realized.

Further limitations of the physical dimensions are given by the width of the laser beam available, which provides the coherent light. Here a commercially available beam expander was used, giving a beam of 50 millimeters diameter, with gaussian phase distribution over the aperture. Standard 35 millimeter slides, which could be illuminated quite uniformly with the expanded beam, were used in the input plane.

The laser beam can be made parallel or converging by adjusting the expander telescope. This feature was used to get the first two dimensional Fourier transform of the input transparency, by focusing down the beam with the telescope, according to Figure 5.

Such an arrangement is described by Vander Lugt<sup>(7)</sup> as the "variable scale" Fourier transform system. The input plane  $P_1$  may be moved axially without disturbing the exact Fourier transform relation between plane  $P_1$  and  $P_2$ ; only the scale of the transform is varied. This system has also the advantage of being space invariant in the sense that all the light emerging from lens  $L_1$  falls on the input plane.

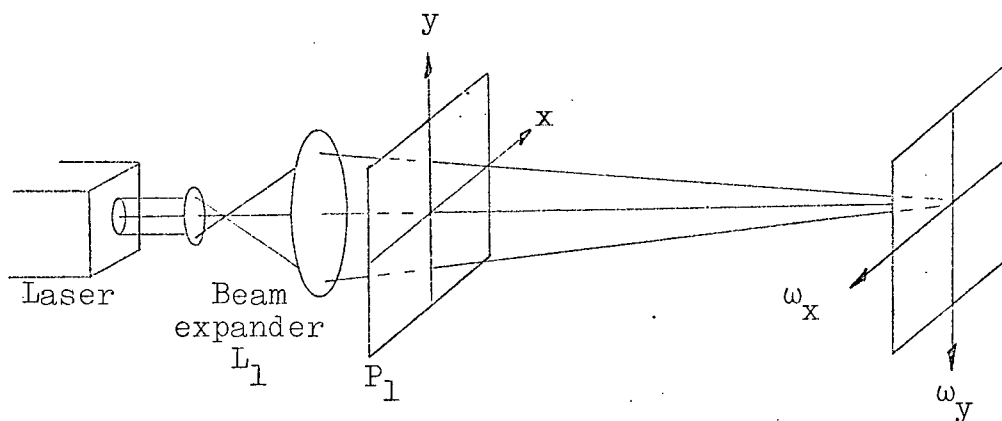


Fig. 5 Variable scale Fourier transformer

A spherical lens, placed right behind the Fourier transform plane, can be used to perform a second transform, giving an approximate one to one imaging onto the output plane. Two cylindrical lenses, inserted at the appropriate places make the system one-dimensional. The basic setup is shown in Figure 6.

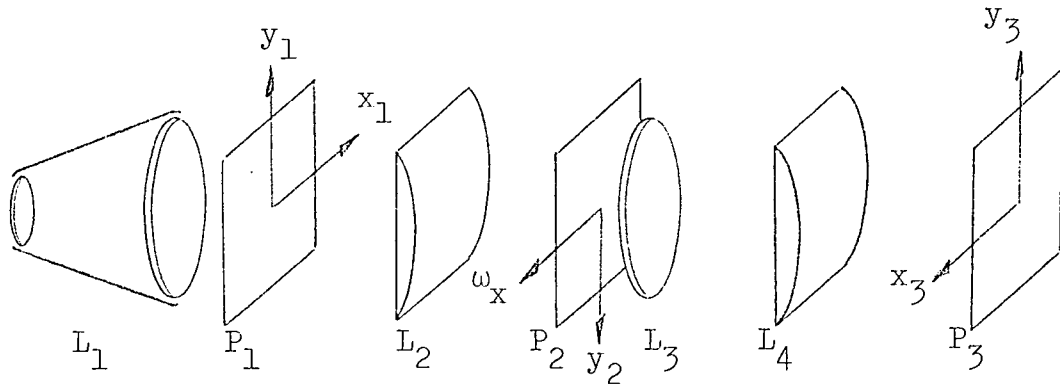


Fig. 6 Basic optical system

### 3.2 Calculations

The computations of the physical dimensions of the system according to Figure 6 will be based on the few desirable properties and given dimensions discussed above, such as size of input picture, beam width, imaging conditions, size of Ronchi rulings.

Let us first determine the diffraction length needed to get the output pictures well separated. The 500 lines per inch Ronchi rulings will be used to perform the spatial frequency sampling, and 1:1 imaging is assumed. This dimension will give us an idea of the total length of the final system. The general equation for the intensity distribution at a point behind a grating according to Figure 7 is given by equation 3.1<sup>(8)</sup>.

$$I(p) = \frac{s^2 L}{\lambda} \frac{\sin \frac{kNd p}{2}}{\sin \frac{k d p}{2}} \quad 3.1$$

where  $p = \sin \theta - \sin \theta_0$  3.2

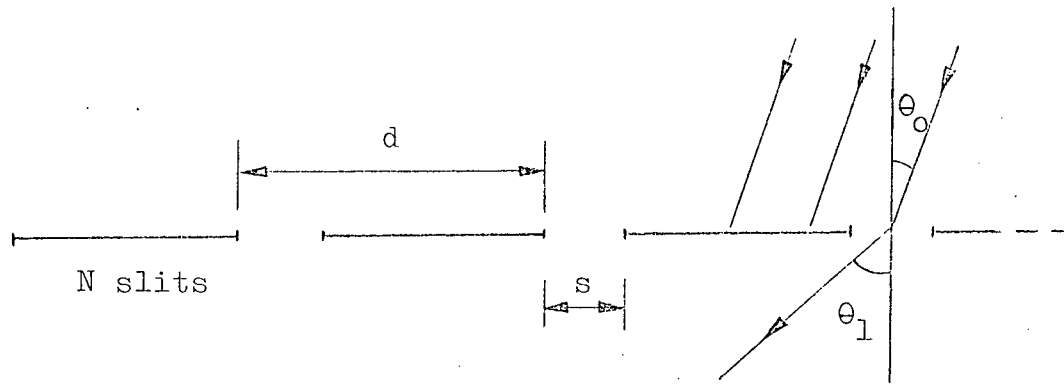


Fig. 7 Diffraction grating

$L$  is the length of a slit.  $k = 0, 1, 2 \dots$

The intensity distribution  $I(p)$  will have maxima due to the period  $d$  of the grating, represented by the first bracket in equation 3.1. These maxima will occur at

$$p = \frac{m\lambda}{d} \quad (m = 0, \pm 1, \pm 2 \dots) \quad 3.3$$

$m$  is the order of interference, it represents the path length difference in wavelengths in the direction of the maximum, from corresponding points in neighbouring slits. The first order maximum occurs at  $p = \frac{\lambda}{d}$ .

In our case we have  $\theta_0 = 0$ , which means that the light is normally incident on the grating.

$$p_1 = \sin\theta_1 = \frac{\lambda}{d} \quad 3.4$$

$\theta_1$  is the angle of the first order diffracted picture with respect to the zero order picture on the optical axis. We may replace  $\sin\theta_1$  by the lateral separation  $b$  of the first order picture, divided by the diffraction length  $l$  of the system.

$$\sin\theta_1 = \frac{b}{l} = \frac{\lambda}{d} \quad 3.5$$

We are now able to determine the diffraction length  $l$  from the given dimensions  $b$ ,  $d$ , and  $\lambda$ .

$$b = 35 \text{ mm}$$

$$d = \frac{25.4}{500} \text{ mm}$$

$$\lambda = 632.8 \cdot 10^{-6} \text{ mm} \quad \underline{l = 2.8 \text{ m}}$$

If we want to accommodate the whole parallel beam of 50 mm diameter,  $l$  comes out to be 4 meters. This value was used in the actual system.

The 35 mm picture in input and output plane corresponds to a television picture scanned by an electron beam, to give an electronic signal of a certain bandwidth. The standard television system used here has 525 lines, of which 21 are used for field blanking; this leaves 504 active lines. The time for one line scan is 63.5  $\mu\text{s}$ , of which 10.8  $\mu\text{s}$  are line blanking time, leaving 52.7  $\mu\text{s}$  for one active line.

Introducing a Kell factor of 0.73, the vertical resolution of the system is 368 lines per screen height. A 4 to 3 aspect ratio results in 490 lines horizontal resolution. These 490 lines are television lines, corresponding to 245 complete cycles black - white, which is the standard used to define resolution of film, and also the spatial frequency.

245 full cycles (in the worst case) are scanned by the television system in 52.7  $\mu\text{s}$ . This leads to a highest necessary bandwidth of the television channel:

$$f_{\max} = \frac{245}{52.7 \times 10^{-6}} = 4.65 \text{ MHz} \quad 3.7$$

To summarize, 245 lines (black - white cycles) across a television picture correspond to a frequency of 4.65 MHz of the video signal. In the optical system described here, this is equivalent to a spatial frequency of 245 lines per 35 mm, according to the chosen picture size.

We recall equation 2.4, which relates the scale of the spatial frequency plane with the physical dimensions of the optical processing system.

$$\omega_x = \frac{-2\pi x}{\lambda F} \quad \omega_x \text{ in radians per unit length} \quad (2.4)$$

To convert into the spatial frequency  $f_x$ , we divide by  $2\pi$ . The highest spatial frequency in our optical system should fall inside an area in the Fourier transform plane given by the size of the Ronchi rulings. 500 line rulings are made in a size of one by two inches, with the lines parallel to the short side. Therefore, for the lateral displacement of the of the highest spatial frequency component from the dc centre line somewhat less than one inch can be allowed. From Figure 6 and the 1 to 1 imaging condition we find that the diffraction length of the output section is also the focal length of the first Fourier transforming lens  $L_1$ . We now can determine the point in the spatial frequency plane, which corresponds to the upper limit of 4.65 MHz actual bandwidth of a video signal, or 245 lines per 35mm spatial frequency, i.e., 7 lines per millimeter.

$$x_1 = \frac{l \cdot 2\pi\lambda f_{\max}}{2\pi} = 17.5 \text{ mm} \quad 3.8$$

$x_1$  is therefore well within the limit of one inch or 25.4 mm given by the size of the Ronchi ruling.

From 3.8 we now find that 1 millimeter in the spatial frequency plane corresponds to  $\frac{7}{17.5} = 0.4$  lines per mm. This is equivalent to an actual signal frequency  $f_1$

$$f_1 = \frac{f_{\max}}{x_1} = 266 \text{ kHz} \quad 3.9$$

The spatial frequency plane is sampled by the Ronchi ruling at an interval  $d$ , which corresponds to a sampling interval  $\Delta f$  in actual signal space.

$$\Delta f = f_1 d = 13.5 \text{ kHz} \quad 3.10$$

Taking the approach from the diffraction theory, we can calculate the spacing of some grating lines, which would correspond to separated output pictures at the chosen diffraction length of 4 meters. From equation 3.5 we have

$$\sin\theta = \frac{b}{l} = \frac{\lambda}{d_{\max}} \quad d_{\max} = \frac{\lambda l}{b} \quad 3.11$$

With  $l = 4 \text{ m}$ ,  $b = 35 \text{ mm}$ ,  $\lambda = 632.8 \cdot 10^{-9} \text{ m}$ , we get  $d_{\max} = 0.072 \text{ mm}$ . Converting into frequency, this corresponds to a sampling interval  $\Delta f_{\max}$

$$\Delta f_{\max} = f_1 d_{\max} = 19 \text{ kHz} \quad 3.12$$

The sampling theorem implies that the sample interval

has to be smaller or equal  $\frac{1}{T_m}$ , with  $T_m$  being the duration of the time limited signal. The time duration  $T_m$  for one line scan in the actual television system is 52.7  $\mu$ s. The necessary sampling interval therefore becomes

$$f_{\max} = \frac{1}{T_m} = 19 \text{ kHz} \quad 3.13$$

This is the same result as obtained from diffraction theory.

The 500 line per inch Ronchi rulings used here, having a spacing equivalent to 13.5 kHz in the 4 m long system, somewhat oversample the spatial frequency plane. This was introduced deliberately by taking 4 m as the diffraction length between Fourier transform and output plane, to ensure a full beam diameter separation. The system could be shortened to the absolute minimum of 2.8 meters, if only 35 mm separation were desired.

### 3.3 The liquid cell

An empty transparency, i.e., a piece of transparent celluloid, in the input plane  $P_1$  of the optical system of Figure 6 produces a great amount of noise in the Fourier transform plane  $P_2$ . The cause of this noise is interference due to the uneven film surface, which acts in the coherent illumination as a phase modulator.

This undesired effect can be greatly reduced by a liquid cell, shown schematically in Figure 8.

The uneven film transparency is immersed in a liquid, which is contained in a box made out of optically flat glass. The liquid has to be of the same refractive index as the film material, which is around 1.5, so that a change in refractive index only

occurs at the optically flat glass surfaces. Several components were tested for the liquid, with pure turpentine giving the best results. A demonstration of the effectiveness of the liquid cell is given in section 4.3.

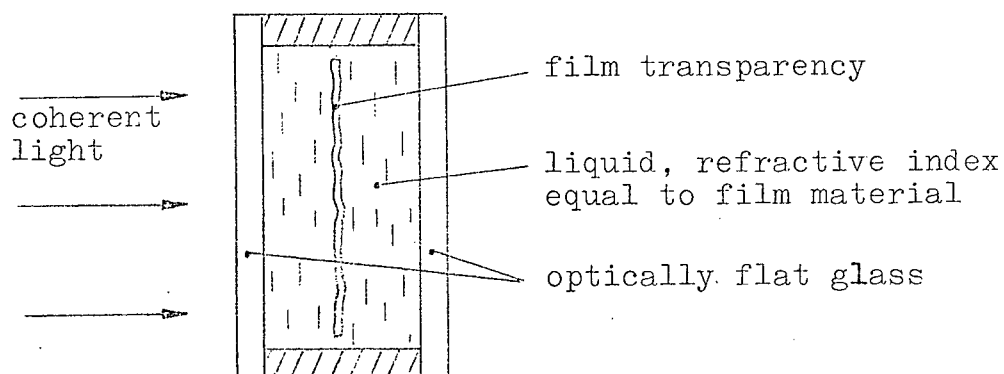


Fig. 8 Liquid cell

### 3.4 Frequency sampling arrangement

To sample the spatial frequency plane at regular intervals, 2 Ronchi rulings were used, providing a variable slit width of 50/50 black, transparent to 100% black. One ruling was fixed-mounted, while the other one was laterally movable by a fine adjusting screw. A thin oil film between the two ruled surfaces enabled them to slide easily on each other. Figure 9 shows the arrangement of the sampling ruling schematically.

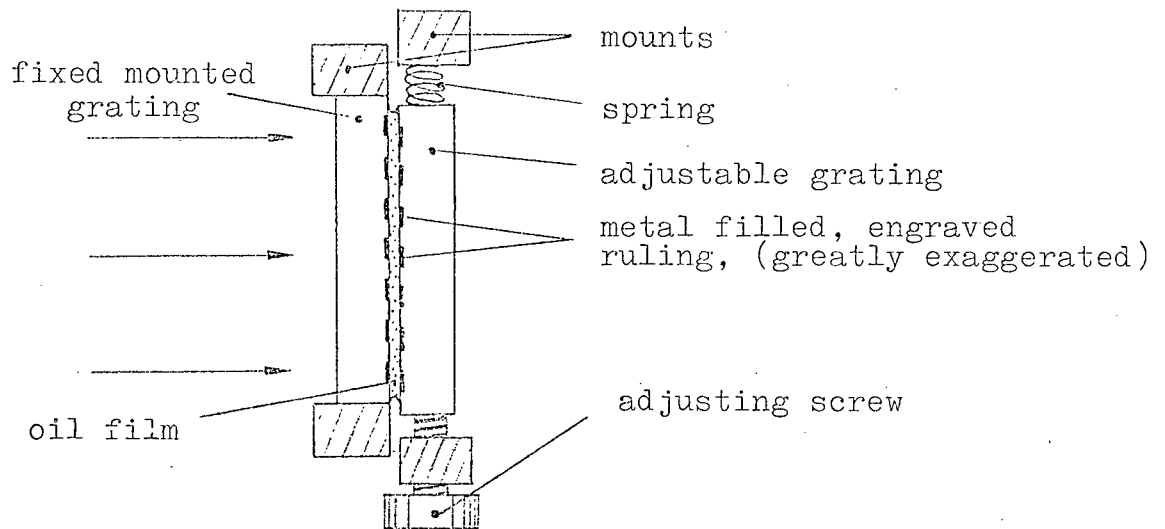


Fig. 9 Adjustable sampling grating

### 3.5 Description of the system

In the actual system of Figure 10 a two meter focal length lens is used as the second Fourier transforming lens, and it is placed right behind the spatial frequency plane  $P_2$ , 4 meters from the input plane and 4 meters from the output plane. This arrangement gives a 1 to 1 imaging. It is easily converted into a one-dimensional system by introducing the two cylindrical lenses  $L_2$  and  $L_4$ . The focal length of these two lenses is not critical as long as  $L_3$ , the spherical lens, is placed right behind the Fourier transform plane, thus being of almost negligible effect on the imaging condition between Fourier transform plane and output plane. The standard equation 3.14, relating the imaging distance  $B$  and the object distance  $G$  with the focal length  $F$  of a lens, may be applied to calculate the dimensions related with the cylindrical lenses  $L_2$  and  $L_4$ .

$$\frac{1}{F} = \frac{1}{B} + \frac{1}{G} \quad 3.14$$

Their focal lengths have to be shorter than one meter, to ensure an imaging solution within the available 4 meters total distance. A focal length of 0.8 meters was chosen for both lenses  $L_2$  and  $L_4$ , giving approximately 3 to 1 imaging between the y-direction of input and Fourier transform plane, and 1 to 3 enlarging from Fourier transform to output plane. The one-dimensional Fourier transform is therefore compressed in the y-direction, and thus fits easily inside the one inch vertical space limit given by the Ronchi ruling.

Slight offset of the lens  $L_3$  from the exact half distance between input and output plane may be compensated by asymmetrical arrangement of the cylindrical lenses, but only in a limited region. For an exact calculation of the general asymmetrical case the equation 3.15<sup>(8)</sup> for a two lens system should be used for the output section.

$$\frac{1}{F} = \frac{1}{F_1} + \frac{1}{F_2} - \frac{H}{F_1 F_2} \quad 3.15$$

$F_1$  and  $F_2$  are the focal lengths of the two lenses,  $H$  is their separation. For lenses in contact, ( $H = 0$ ), this equation reduces to a simple addition of the powers of the lenses.

In practice, the symmetrical system was found to be easiest to handle, because alignment procedures soon get very difficult with an asymmetrical setup, due to the large number of variables involved and the physical dimensions of the system.

Figure 10 shows schematically the final system.

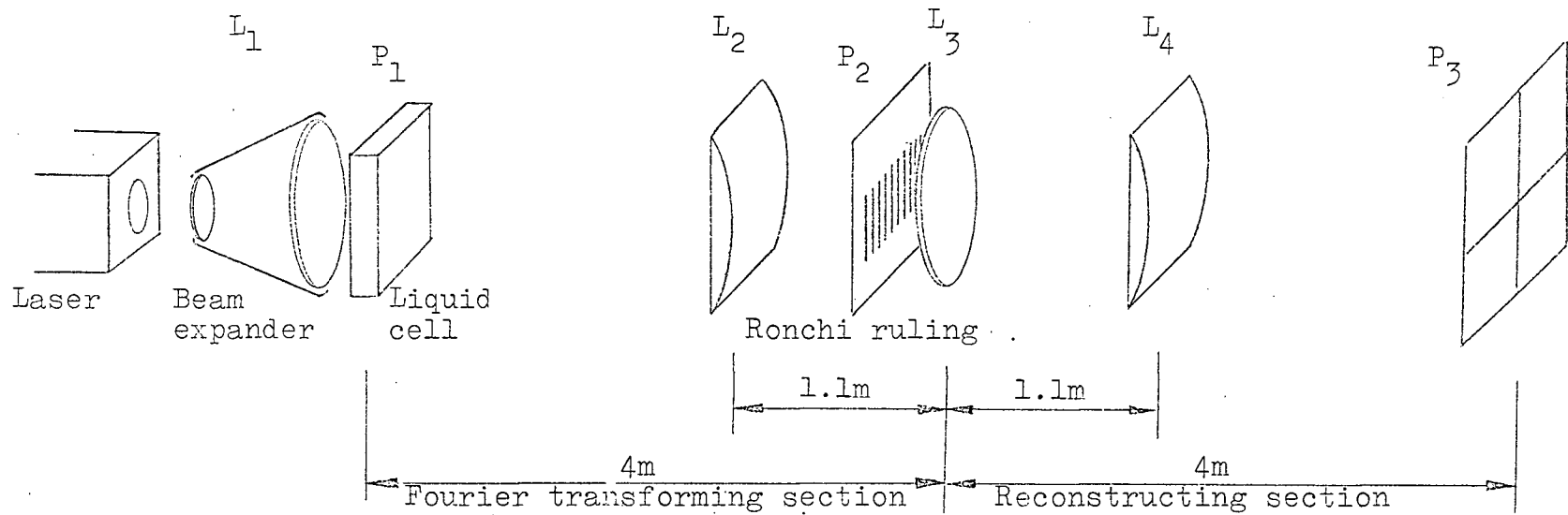


Fig. 10 The final optical system

- $L_1$ : Beam expander telescope, adjusted to  $F = 4\text{m}$ , 50mm diam.
- $L_2$ : Cylindrical lens,  $F = 0.8\text{m}$ , 55mm diameter
- $L_3$ : Spherical lens,  $F = 2\text{m}$ , 55mm diameter
- $L_4$ : Same as  $L_2$

All lenses had to be of excellent quality, ground to within the order of a wavelength. Any kind of surface distortion was readily observable in the output plane. The cylindrical lenses were mounted in rotatable rings to provide easy adjustment of the optical axis.

The scale of the spatial frequency plane  $P_2$  in this system was as calculated under 3.2., i.e., 1 mm in the spatial frequency plane corresponds to 0.4 lines per mm in the input plane, or to 266 kHz of an actual video signal.

## 4. FOURIER TRANSFORMS AND SPATIAL FILTERING

### 4.1 Two-dimensional Fourier transforms

The first section of the optical system according to Figure 10 is converted into a two-dimensional Fourier transforming arrangement by removing the cylindrical lens  $L_2$ . Figures 11 and 12 show the ROWI test chart and the corresponding two-dimensional Fourier transform as observed in plane  $P_2$ . The center part, representing the dc and low frequency content of the transformed picture, had to be somewhat overexposed, to show the weaker parts of the light distribution.

Plane  $P_2$  may be labelled in spatial frequency by a polar co-ordinate system  $\omega_p(r, \varphi)$ , with origin in the central dc point. The concentric fringe pattern represents the transform of the rings in the original, with strong harmonics at the spatial frequencies corresponding to the width and spacing of the rings. The repetitive dot patterns are due to spatial detail in the respective directions. Figures 13 and 14 show an off center detail of the same chart and its transform. Note here especially the strong, widely-spaced harmonics in the horizontal and vertical directions, corresponding to oval clusters of fine vertical and horizontal lines.

Although these transforms are not of primary interest for investigations of a one-dimensional television signal, they show some basic characteristics of the performance of an optical system. For example, they show clearly that only a small part of the total area of the frequency plane is really occupied by the light distribution, at least for a two tone picture like the ROWI chart.

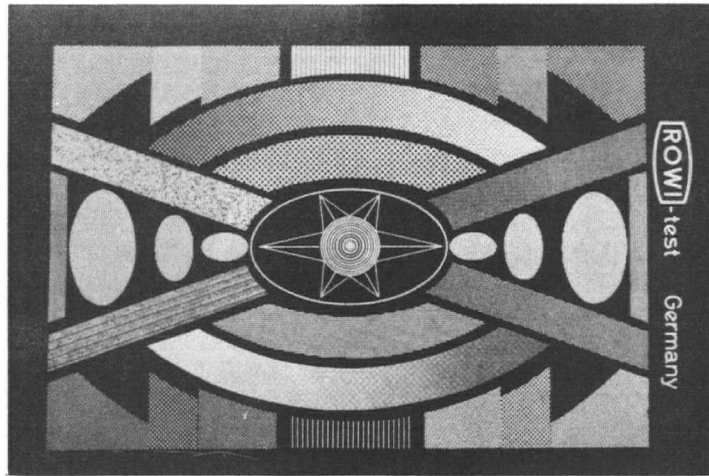


Fig. 11 ROWI test chart

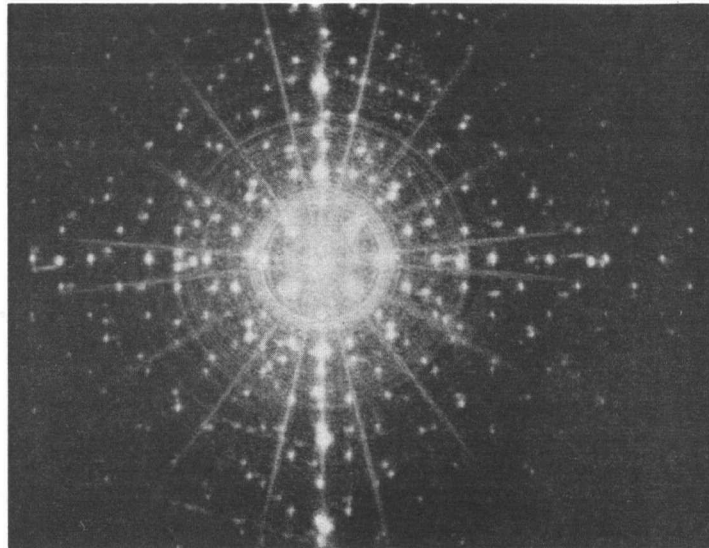


Fig. 12 Two-dimensional Fourier transform of Fig. 11 (Center part overexposed)

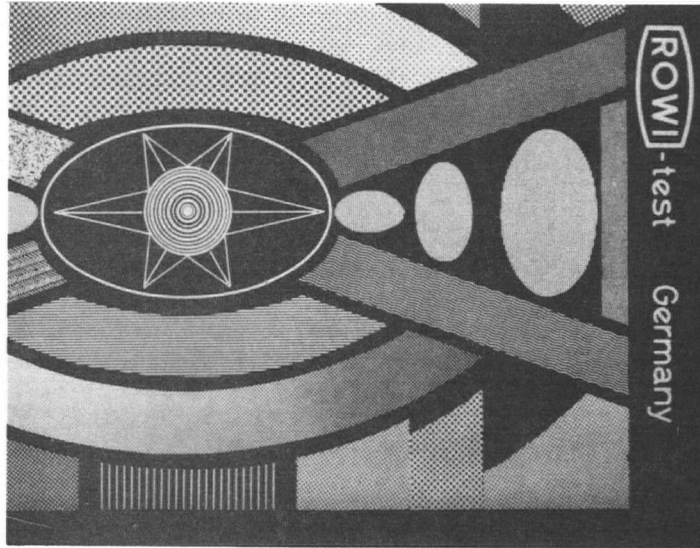


Fig. 13 Detail of ROWI test chart

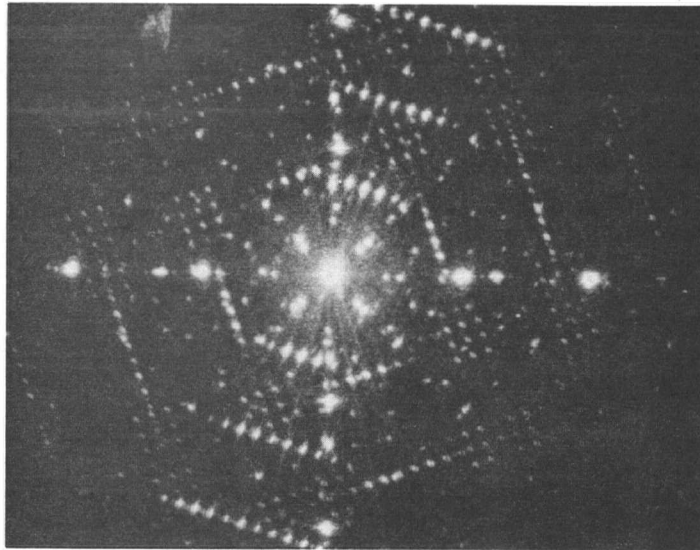


Fig. 14 Two-dimensional Fourier transform  
of Fig. 13

Furthermore, the analogy between the Fourier transform plane in the optical system and the hologram plane of a Fraunhofer diffraction hologram may be mentioned here again. By superimposing a reference beam on the Fourier transform we get a hologram of the input picture, which could be recorded on an appropriate photographic emulsion. The reference beam in holography is needed to get a recording of the phase distribution in the hologram plane by means of interference, because photographic emulsion only responds to intensity and not to phase. A hologram then is able to fulfill the condition that the phase information also has to be retained in the Fourier transform plane if further processing of the signal, e.g., a second Fourier transform producing a reconstruction of the original, is to be performed. (7)

On the other hand, filters produced by holographic techniques may be introduced in the Fourier transform plane to achieve complex filtering, as has been done in some pattern recognition experiments. (6)

#### 4.2 One-dimensional Fourier transforms

Inserting the cylindrical lens  $L_2$  at the appropriate place into the system of Figure 10, we obtain a one-dimensional, multichannel Fourier transform arrangement. Now an imaging condition relates the y-axis of the planes  $P_1$  and  $P_2$ , while the x-axis is unchanged and still governed by the Fourier transform relation.

Figure 15 shows the one-dimensional transform of the central part of the ROWI test chart; Figures 16 and 17 show the Marconi resolution chart No. 1 and its Fourier transform. Here

it is easy to relate the light distribution of the Fourier transform to the original picture. As it is well known from the grating equation 3.3, the separation of the secondary maxima of a diffraction pattern is inversely proportional to the spacing of the grating; the same relation may also be derived from the definition of the spatial frequency (equation 2.4). We are thus able to calibrate Figure 17 very easily in a spatial frequency scale, with respect to the original test chart. The intensity maxima for the different line spacings from 100 up to 600 lines per picture width are clearly visible, as well as the sloping lines corresponding to the fanning-out lines in the center part of the original.

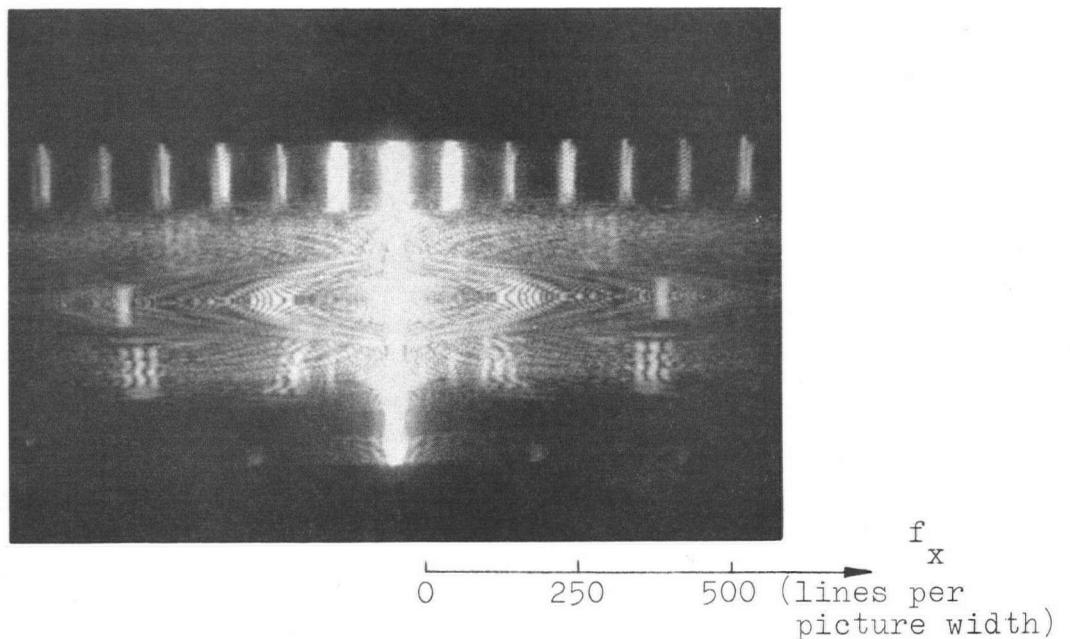


Fig. 15 One-dimensional Fourier transform of ROWI test chart (center part)

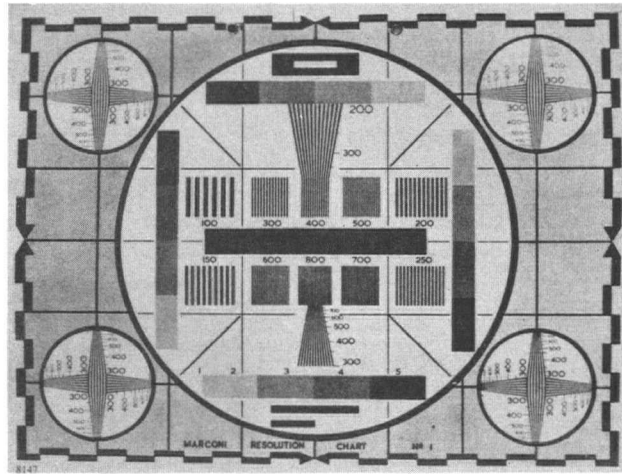
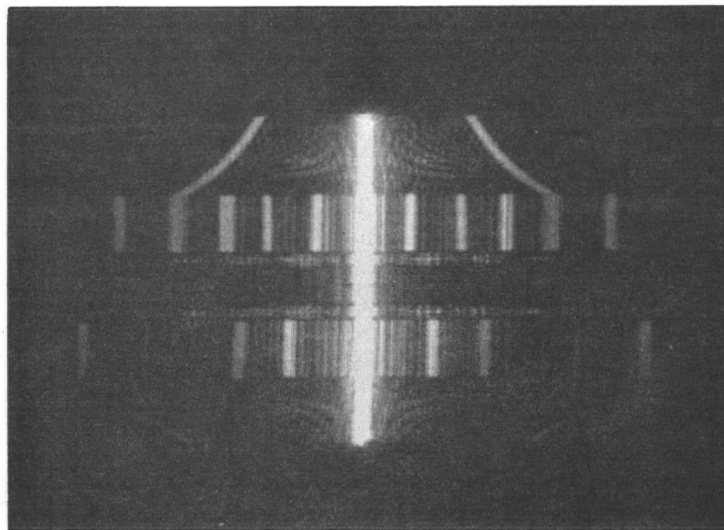


Fig. 16 Marconi resolution chart No. 1



0 200 400 600  $f_x$   
 (lines/picture width)

Fig. 17 One-dimensional Fourier transform of  
 Marconi chart (centre part)

### 4.3 Relation to video signal

A television signal is produced by scanning a picture, line by line, at a certain rate. As it is well known,<sup>(3)</sup> this leads to a concentration of the power in the frequency spectrum at the harmonics of the line repetition frequency. This fact is based on the supposition of a time limited signal of the duration of one line scan, or a sequence of similar signals of equal length.

In our optical system we find an exact equivalent to the real time signal. The one-dimensional system treats the input picture line by line, giving the immediate Fourier transform of each line. The horizontal axis of the picture is labelled time, and the picture width then determines the time for one line scan, which, in the Fourier transform plane, will give rise to power concentrations at the harmonics of the spatial frequency corresponding to the picture width.

The aperture given by an empty frame as the input picture produces a Fourier transform as shown in the Figures 18 and 19. This is the well known pattern of a Fraunhofer diffraction at an aperture in optics.<sup>(8)</sup> Here the secondary maxima are the analogue of the maxima in the frequency spectrum of a television signal, spaced at intervals corresponding to the inverse line duration.

The effect of the liquid cell described in section 3.3 is demonstrated by the Figures 20 and 21, both showing the Fourier transform of an aperture with an empty transparency of clear film material introduced. The severely disturbed line pattern of Figure 20 is restored in Figure 21, which was taken with the same transparency, immersed in the liquid cell.

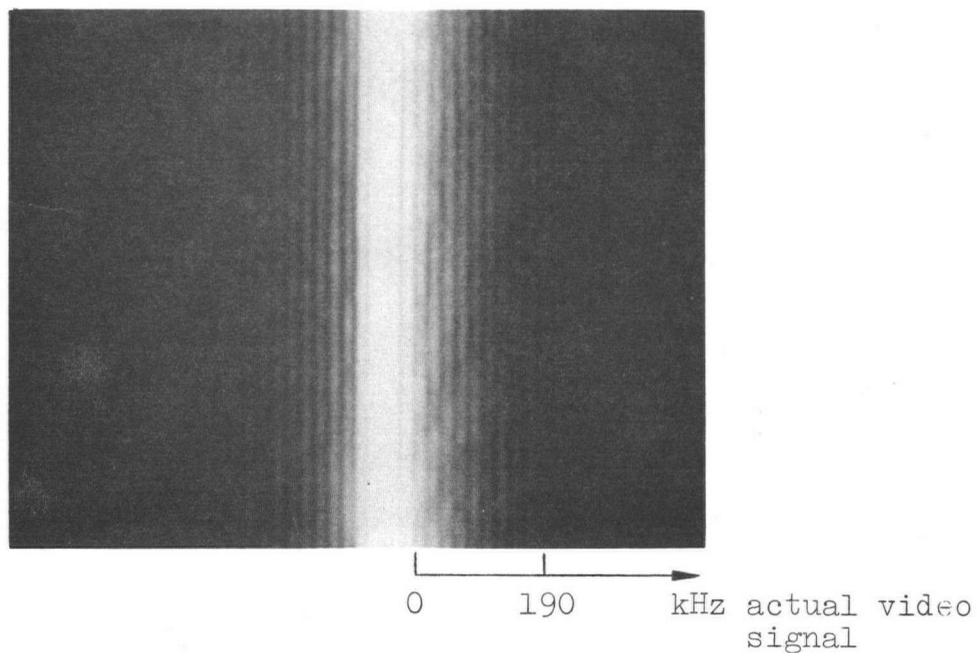


Fig. 18 One-dimensional Fourier transform of an aperture (Center part overexposed)

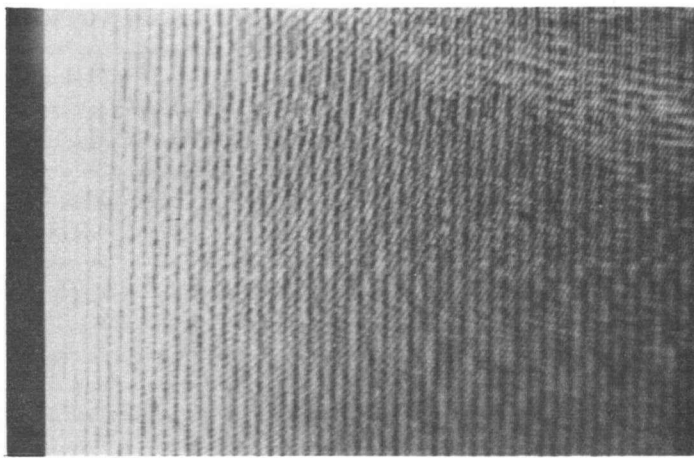


Fig. 19 Part of the same transform as in Fig. 18, only showing higher spatial frequencies. Line spacing equivalent 19 kHz actual video signal. (Fringe pattern due to lens used for enlargement in photographic process)

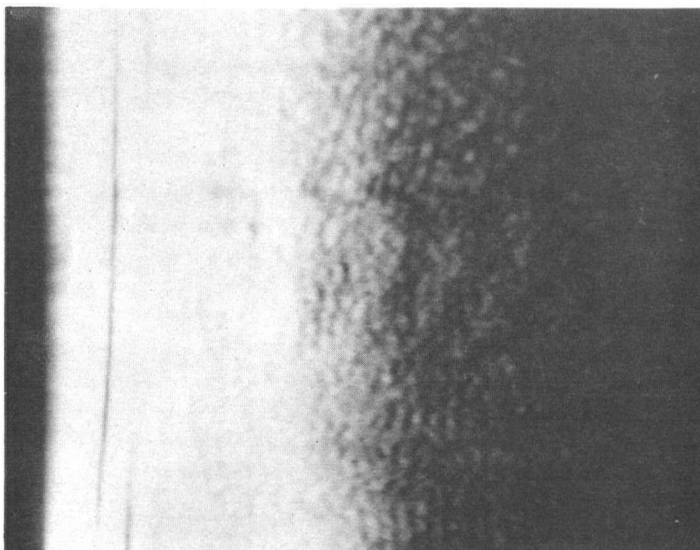


Fig. 20 Fourier transform of aperture with empty transparency

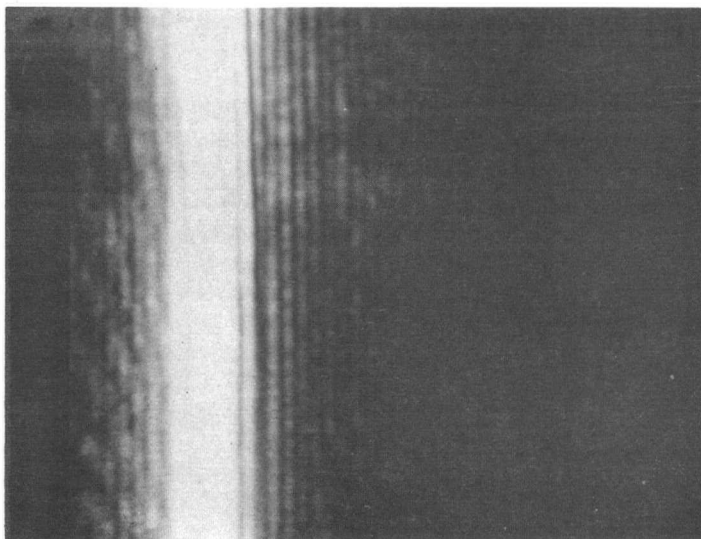


Fig. 21 Fourier transform of aperture with empty transparency in liquid cell

#### 4.4 Frequency sampling

The string of separated output pictures produced by the frequency sampling is shown in Figure 22. The input picture was a 35 mm frame containing the center part of the ROWI test chart. As calculated in section 3.2, the rulings are able to sample a 50 mm picture without ambiguity, i.e., without producing overlapping outputs.

Figure 23 shows the output of the system without the sampling ruling. The rounded off edges are due to the small size lens used for enlargement in the photographic process.

Figure 24 shows the same image of the output plane, but with the rulings inserted and adjusted to a quite narrow slit width of approximately 15 to 1 opaque to transparent ratio. The effect on the output picture is merely a decrease in overall intensity (compensated here by longer exposure of the photography). Some slight degradations are caused by imperfections in the rulings, only visible under a microscope, and are independent of slit width. Figure 24 thus is a very convincing demonstration of the frequency sampling theorem.

Figure 25 shows an enlarged part of the Fourier transform plane with the sampling grating, adjusted to the same slit width as used for Figure 24. All sampling lines are of equal width; the apparent broadening of some bright lines is due to overexposure of these lines, which was necessary to show the weaker parts.

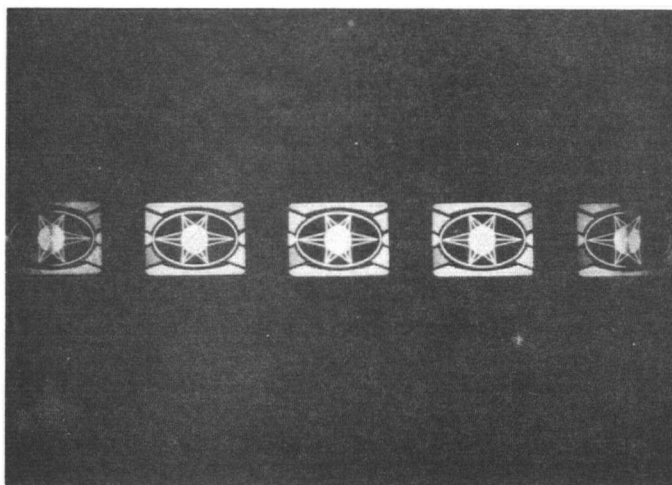


Fig. 22 String of output pictures after frequency sampling

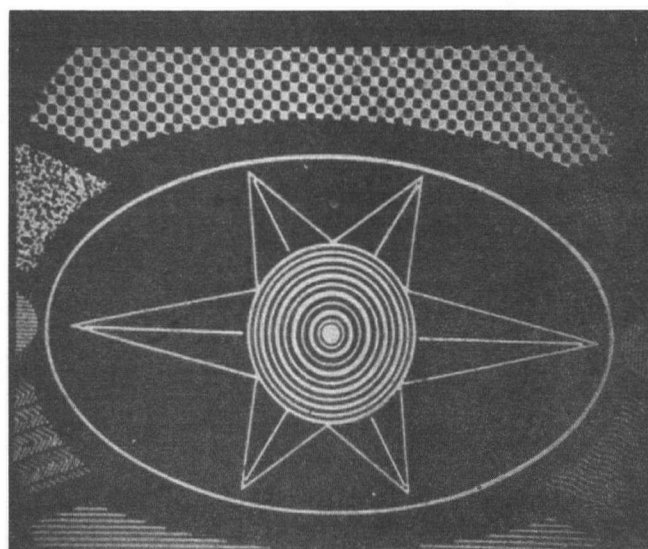


Fig. 23 Single output picture without sampling

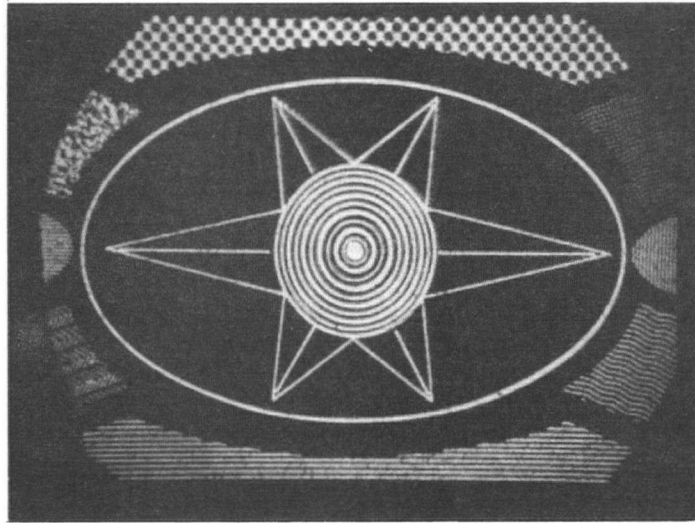


Fig. 24 Central (zero order) output picture  
after frequency sampling

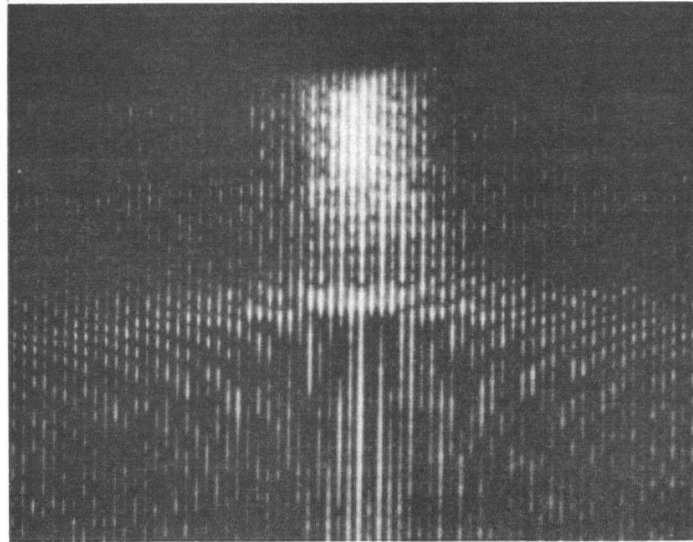


Fig. 25 Enlarged part of sampled spatial frequency  
plane. (Apparent irregular sample width due  
to overexposure)

#### 4.5 Coarse filtering

For the following experiments, for ease of observation, the output plane was viewed by a camera of a closed circuit television system and displayed on a monitor. The picture on the monitor was naturally somewhat degraded, but much more convenient to observe. Figure 26 is a photograph of the output picture of Figure 24, displayed on the monitor.

Some basic properties of the optical system may be shown by very simple, coarse filtering, placing stops in different parts of the Fourier transform plane. The effect of a low pass filter, realized by a 10 mm wide slit in the Fourier transform plane, passing only the central dc and low frequency region, is demonstrated by Figure 27. The difference in resolution of vertical and horizontal lines is apparent. The vertical resolution is not affected by this filter in the one-dimensional transform.

A high pass filter is realized by a stop in the dc region. The effect of a 5 mm wide stop is demonstrated by Figure 28. Horizontal lines are completely lost because of the missing low frequency components.

As it can be seen from Figure 15, the frequency spectrum of the ROWI test chart contains many empty and low intensity spots. A very crude filter, passing only some of the brightest parts of the Fourier transform plane (Figure 29), gives a fairly good reconstruction, shown in Figure 30. Note here, for instance, the perfect reconstruction of the fine checkerboard pattern, which is contained in the string of harmonics at the top of Figure 29. The reduction in bandwidth for this part of the picture is approximately 6 to 1. The lower half of the central ring pattern is re-

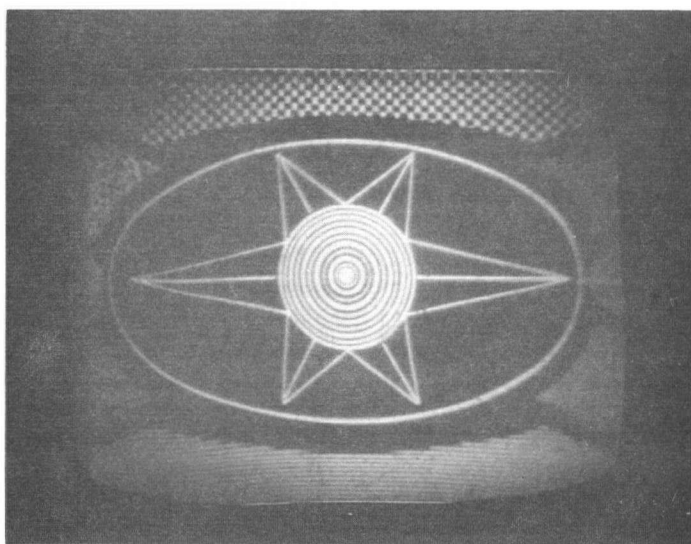


Fig. 26 Output picture displayed on closed circuit television monitor

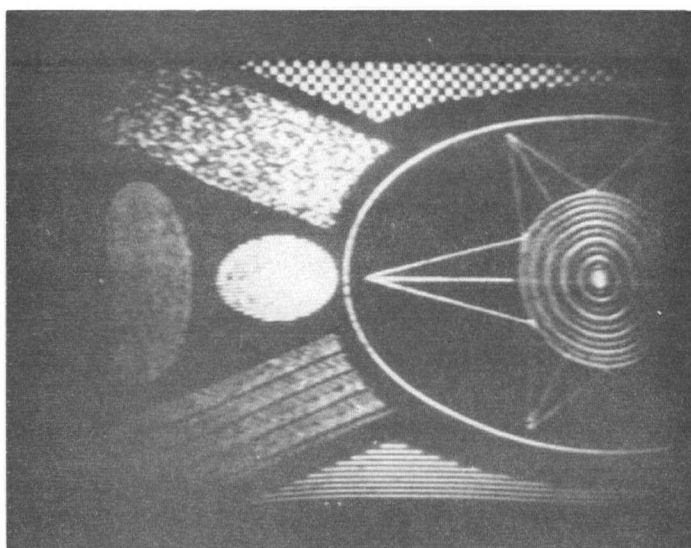


Fig. 27 Effect of low pass filter

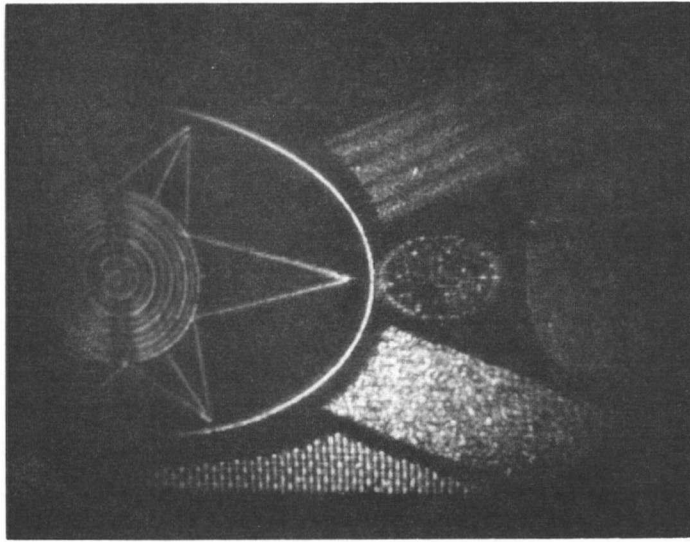


Fig. 28. Effect of high pass filter

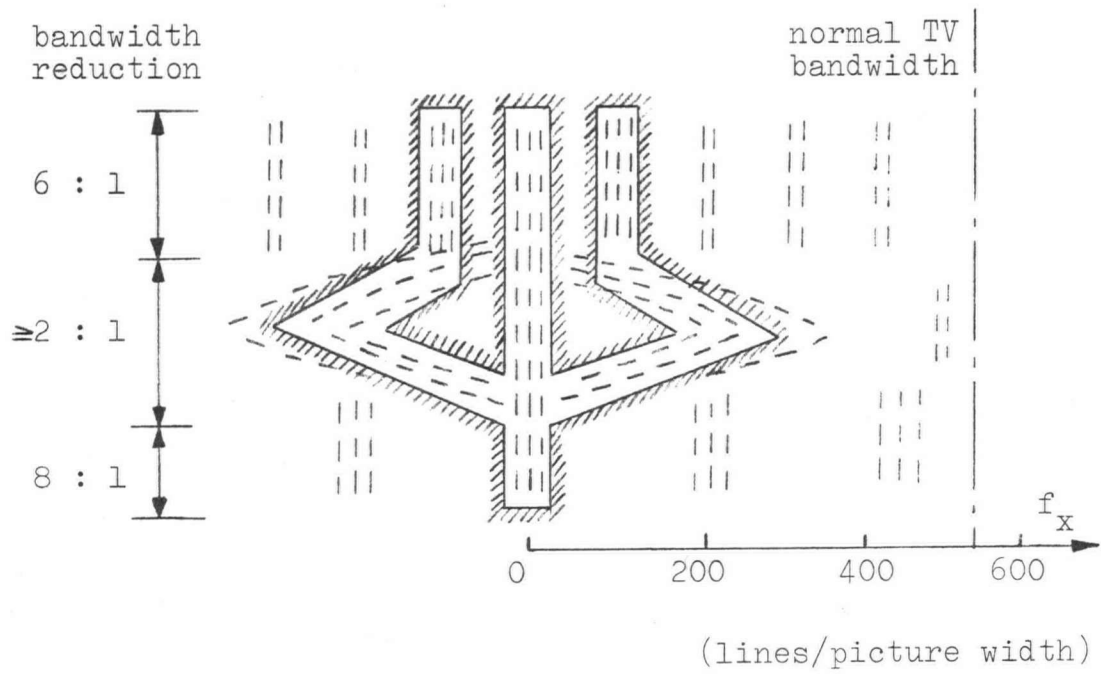


Fig. 29 Mask filter in Fourier transform plane of Fig. 13 (Broken lines mark high intensity regions in spectrum)

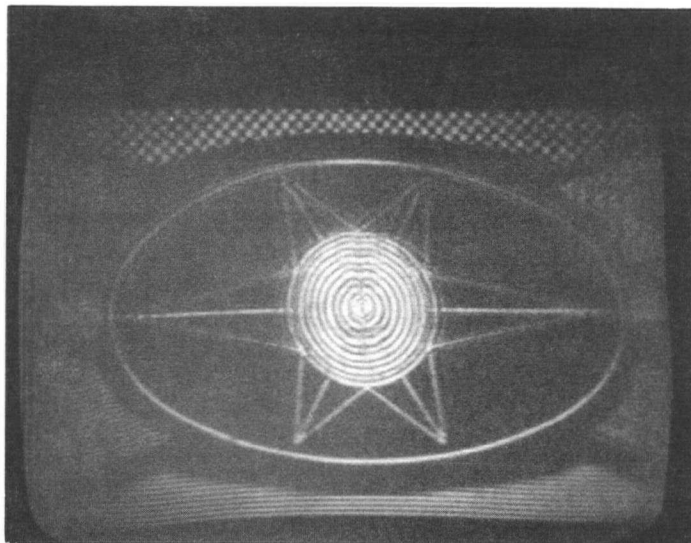


Fig. 30 Output from mask filter of Fig. 29

produced much better than the top half. The two vertical bars in the filter of Figure 29 stop out parts of the Fourier transform, which are essential for the reconstruction of the ring pattern.

In general, the reconstruction is quite good, considering the very rough methods used to realize the mask filter. (It was shaped by eye to match the brightest parts of the spectrum). It seems possible to save transmission bandwidth by omitting all the unused parts of the spectrum of the transmitted signal in a suitable television system.

It is not possible to treat a continuous tone picture in the same way. The spectrum of such a picture (Figure 30) is shown in Figure 31. High spatial frequencies were very low in intensity, (not even recorded on the photograph), and were submerged in noise. Their presence could only be inferred in the reconstruction by masking in the Fourier transform plane. Nothing definite can therefore be said about the actual shape of the Fourier transform

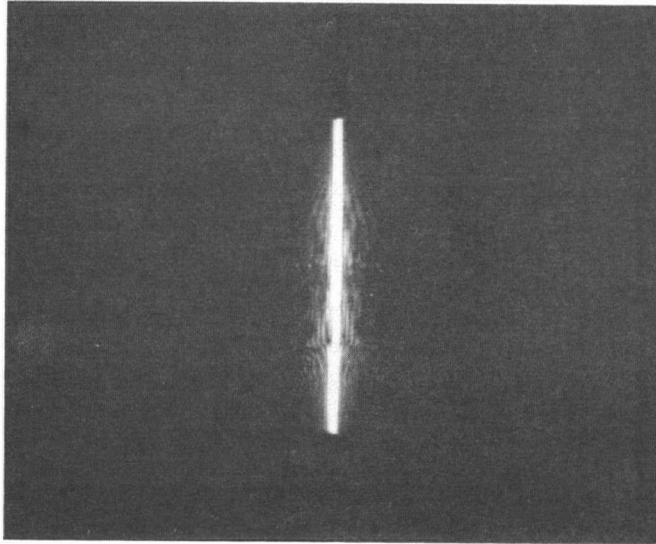


Fig. 31 Fourier transform of a continuous tone picture ("Face" Figure 38)

for this class of pictures.

## 5. SPATIAL FREQUENCY FLICKER EXPERIMENTS

### 5.1 Basic idea

It is well known that image quality is a highly subjective measure. There are quite a number of physiological factors that determine the apparent quality, especially for a real time television picture. It is known, e.g., that a frame repetition as high as 30 per second is unnecessary for most television reproductions, even of fast moving scenes<sup>(9)</sup>. Some savings of transmission bandwidth could be achieved taking advantage of this fact, or of related properties of the human eye.<sup>(10)(11)</sup>

More related to our approach of investigating the spatial frequency domain is the variation in response of the human eye to different spatial frequencies. Measurements of this "static" relationship have been made by several workers<sup>(12)(13)</sup>; the results found by Lowry and de Palma<sup>(14)</sup> seem most widely accepted at this time. (Figure 32)

Normalized response

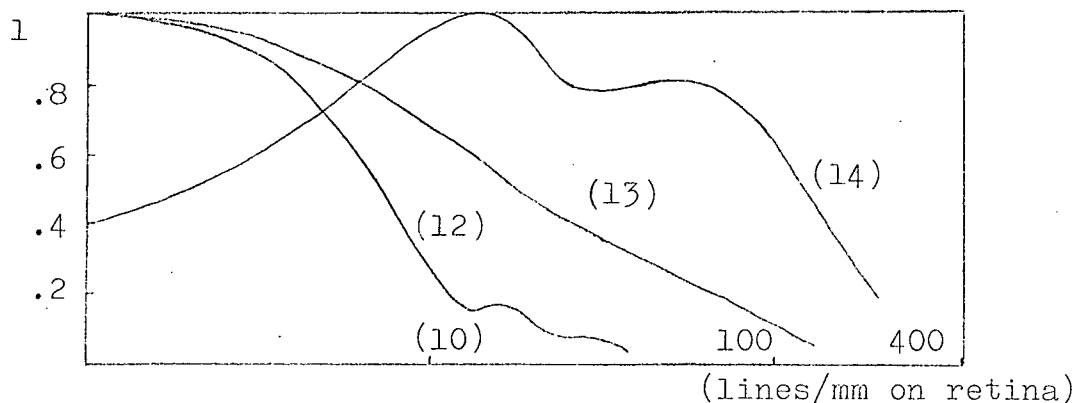


Fig. 32 Sine wave response of the human eye

With respect to a television picture display, one question seems of special interest to us: How is the response of the human eye to spatial frequencies affected by the fact that the picture is presented only part of the time rather than continuously? Or, in other words, what is the critical flicker frequency as a function of spatial frequency? If this "dynamic" characteristic has the same generally negatively sloping relationship for high spatial frequencies as the "static" one, then it could be taken advantage of by presenting the high spatial frequencies of a television display at a lower rate than the actual frame repetition rate. The results of some related investigations<sup>(15)</sup> seem to justify a closer look into that question.

The optical signal processing system may be used quite easily for a study of this problem. The spatial frequencies are readily accessible in the Fourier transform plane. A simple chopping disc may be used to stop out all spatial frequencies above a certain limit temporarily, at a variable repetition rate, thus "flickering" the higher spatial frequency content of a picture. The effect on the picture quality can be judged simultaneously by the reconstruction in the output plane.

## 5.2 Test arrangement

To get some general and reproducible measurements, a picture consisting just of a vertical bar pattern was used here in a number of subjective tests. The setup for these flicker tests is shown in Figure 33. A chopping wheel is rotated by a small dc motor, producing a variable flicker rate of 50/50 on/off time ratio for a part of the Fourier transform plane. The

side band stop blocks out one half of the spectrum, passing only a "dc plus one sideband" signal, which is sufficient to reconstruct the lines of the test picture. The total information is contained in either side of the symmetrical Fourier transform, as for the normal amplitude modulation spectrum. Only one sideband was used in the flicker experiment here, to avoid the necessity of two synchronous chopping wheels for the high spatial frequencies of both sides of the spectrum.

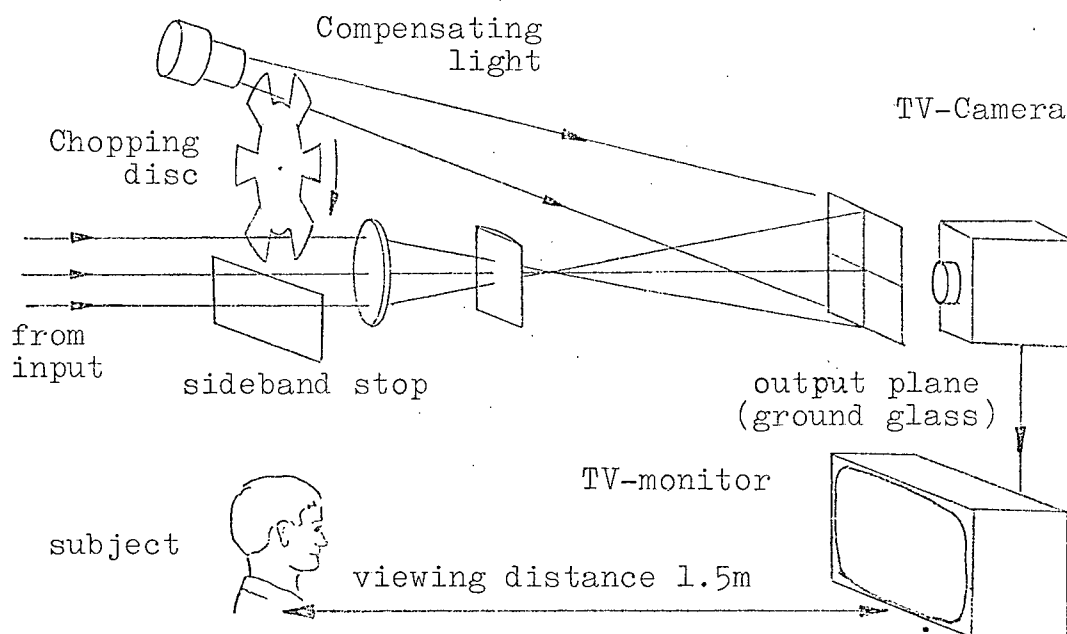


Fig. 33 Flicker test arrangement

The output plane was viewed by means of the television camera and monitor, so that brightness and contrast ratio could be easily adjusted. The secondary flicker introduced by this viewing arrangement is negligible if the set is well adjusted with regard to storage time of vidicon and monitor, and if the flicker introduced by the chopping wheel is not in the same frequency range of 60 per second (half frame rate), which would pro-

duce some beat frequency effects. As it turned out, the critical spatial frequency flicker was always below 30 per second, and no stroboscopic effects were observed.

An auxiliary light was provided by a Zeiss microscope illuminator shining through the chopper disc at the appropriate time. It was found to be necessary to illuminate the output plane during the time when the spatial frequency plane was partially obscured.

The explanation for this seems to be the following: For increasing spatial frequencies, the impression of a grey surface rather than the line structure of the test slide seems to become more and more dominant in the perceived image. Cutting out part of the Fourier transform plane naturally reduces the total intensity in the observed picture by a certain amount. This is perceived as a change in the overall brightness of the picture, i.e., a flicker. Using Biernson's somewhat controversial feedback model of human vision<sup>(16)</sup>, this effect may be explained by the fast response of the spatial average feedback, which also produces the grey impression.

The auxiliary, compensating light, superposed during the chopping time, eliminated this effect, and the eye seemed to concentrate on the line structure again, as can be seen from the results of section 5.3. The intensity of the light was adjusted easily to the necessary value by the focussing system of the Zeiss illuminator.

### 5.3 Results

Using the arrangement of Figure 33, a series of subjec-

tive tests was carried out, with 4 subjects, 3 male and 1 female; their ages ranged from 20 to 28 years. The test persons were asked to judge the image consisting of a vertical bar pattern (50/50 black/white ratio) as "good" and "acceptable", while the flicker rate of the essential first harmonic in the spatial frequency plane was varied. The results of these tests are summarized in the Figures 34 and 35.

The tests were run 3 times, to check the consistency of the judgement. It was found that the results between different runs varied only slightly, mostly by no more than  $\pm 1$  cycle of flicker rate.

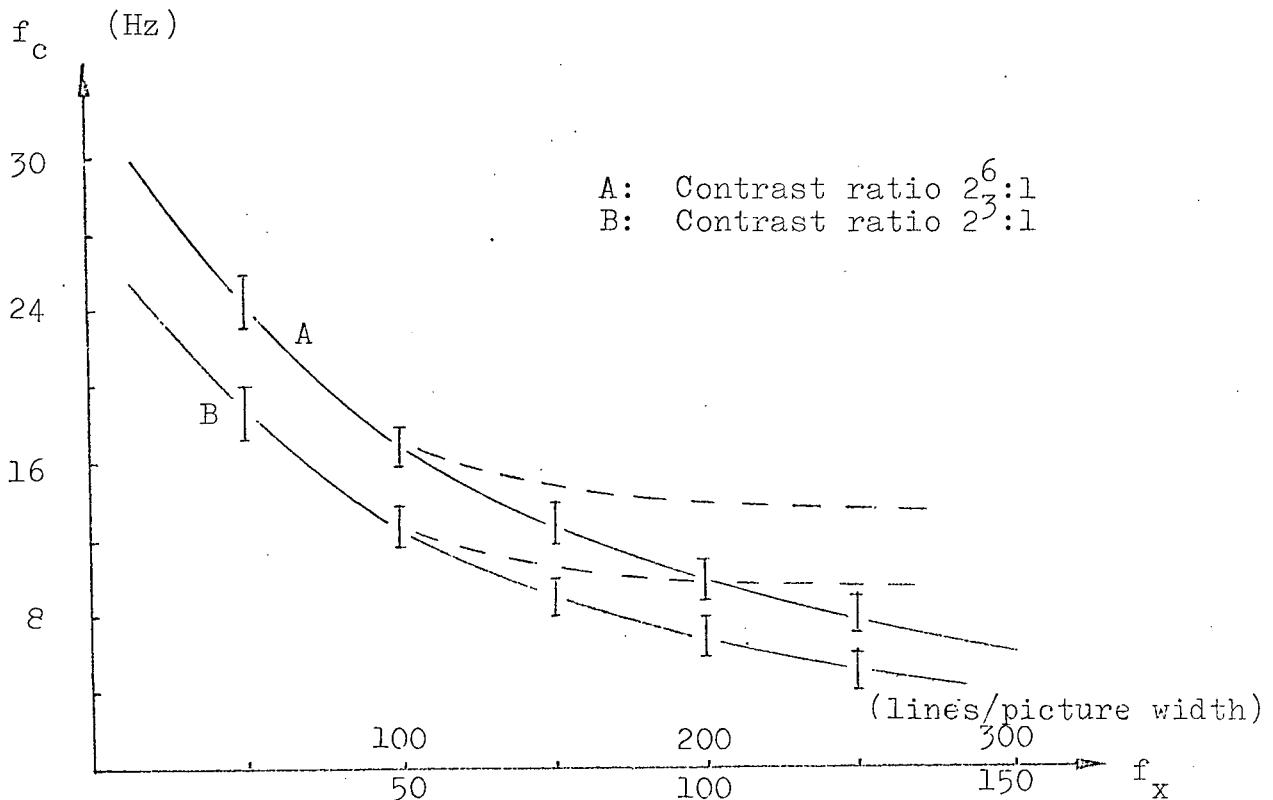


Fig. 34 Critical flicker frequency as a function of spatial frequency for judgment "good".  
 (Broken curve without brightness compensation)

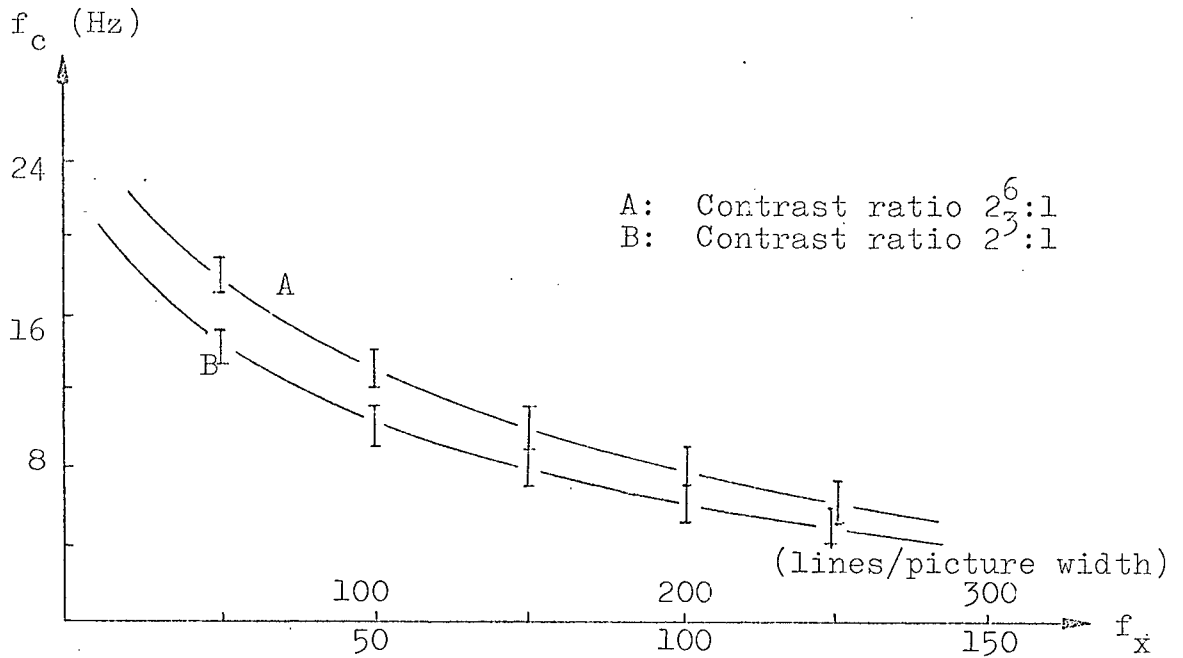


Fig. 35 Critical flicker frequency as a function of spatial frequency for judgement "acceptable"

The contrast ratio of the line pattern was adjusted by measuring the light intensities for peak white and peak black directly on the screen with a light meter. The influence of the contrast ratio on the results is made clear by the curves of Figure 36, which are based on "good" judgements like the curves of Figure 34.

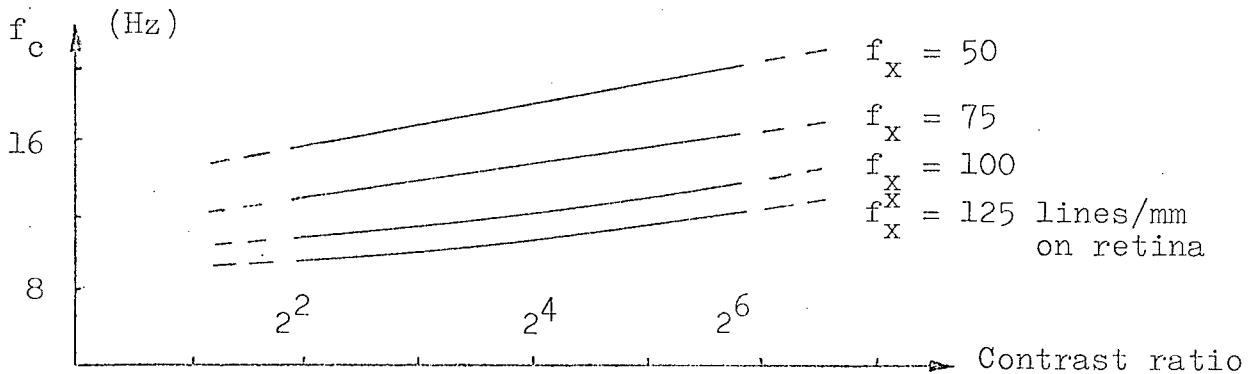


Fig. 36 Critical flicker frequency vs contrast ratio.

The critical flicker frequency appears to be a logarithmic function of the contrast ratio. Only for high spatial frequencies at low contrast ratios is there a slight deviation from the logarithmic behaviour. This may be due to the dominating grey impression received under these conditions.

The background illumination was held at a reduced level of approximately 180 lux. Variations in room illumination from 2 lux to 700 lux were tested, but found to be of negligible influence. A bright background increased the critical flicker frequency very slightly, especially for high spatial frequencies.

The influence of the average brightness of the picture was checked over a 9 to 1 luminance range, from approximately 40 to 350  $\text{cd/m}^2$ . The effect of the contrast ratio dominates the brightness effect by far, but it seems that the critical flicker frequency increases very slightly with increasing brightness. An average screen luminance of 200  $\text{cd/m}^2$  was used for the experiments of Figures 34 to 37.

The influence of the size of the picture area is shown in Figure 37; it is very small also, and lies almost within the uncertainty of about  $\pm 1$  Hz basically inherent in the tests. A trend to increased critical flicker frequency with larger area is noticeable.

A much larger number of tests has to be carried out to get more exact results, but this was beyond the scope of this thesis. Generally, it may be said that the effects of picture area, brightness and background are only small and seem to be consistent with results for total rather than partial flickering found by Foley<sup>(17)</sup>, which show basically logarithmic behaviour.

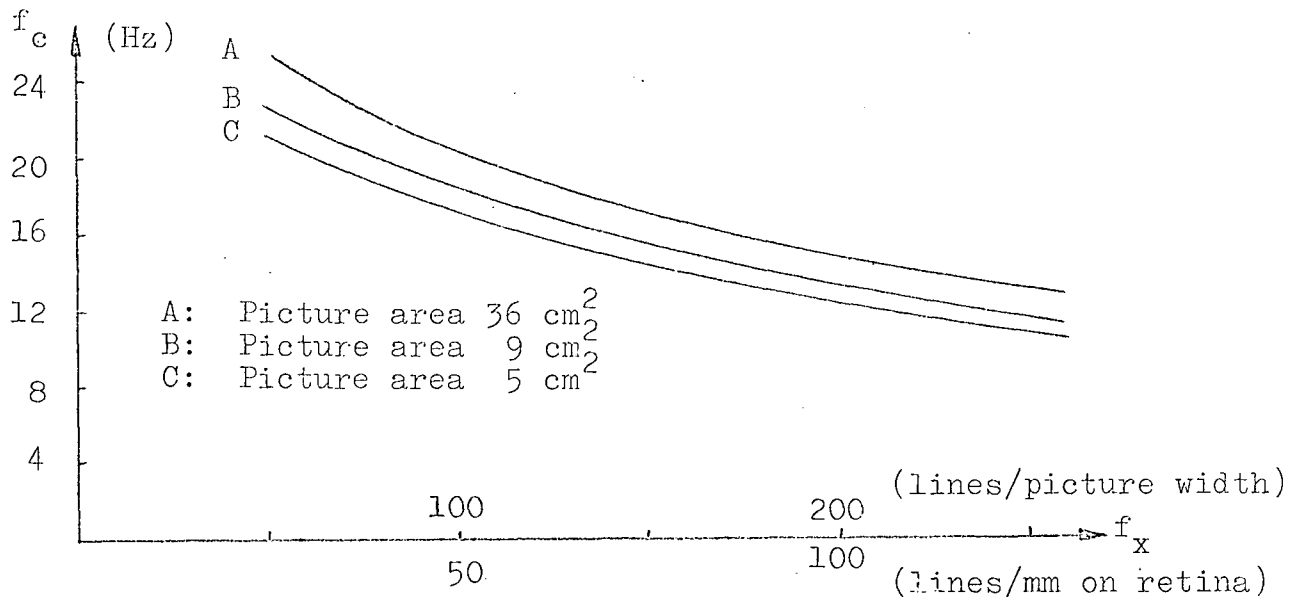


Fig. 37 Critical flicker frequency with picture area as parameter

Finally some subjective quality tests were carried out with the pictures of Figures 38 and 39, flickering the higher spatial frequencies. Here it was not necessary to restore the average brightness during the chopping period; the power of the high spatial frequency components is very low, and no change in average brightness was observed.

The results of these tests are summed up in Figure 40. They show, for example, that the severely bandlimited picture of Figure 41, which resolves only 50 lines per picture width, may be presented alternatively with the original picture (Figure 38) at a rate of 19 Hz, to give a subjectively perfect image. For less bandlimitation, the rate may be decreased below that value.

It can be seen immediately that this fact may be used to save transmission bandwidth in a television system. There is, however, an obvious limit to the compression that can be achieved this way. It is given by the ratio of the total area of Figure 40 to the area under the curves, which comes out to be approximately

3 to 1.



Fig. 38 "Face" (viewed on TV-monitor)

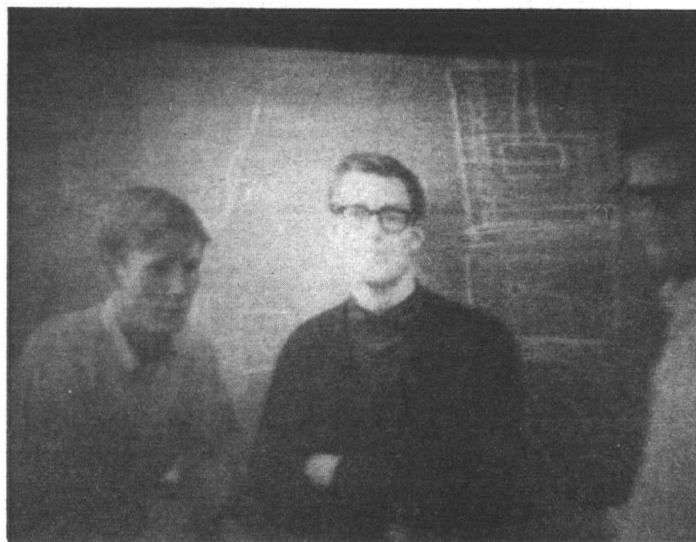


Fig. 39 "Group" (viewed on TV-monitor)

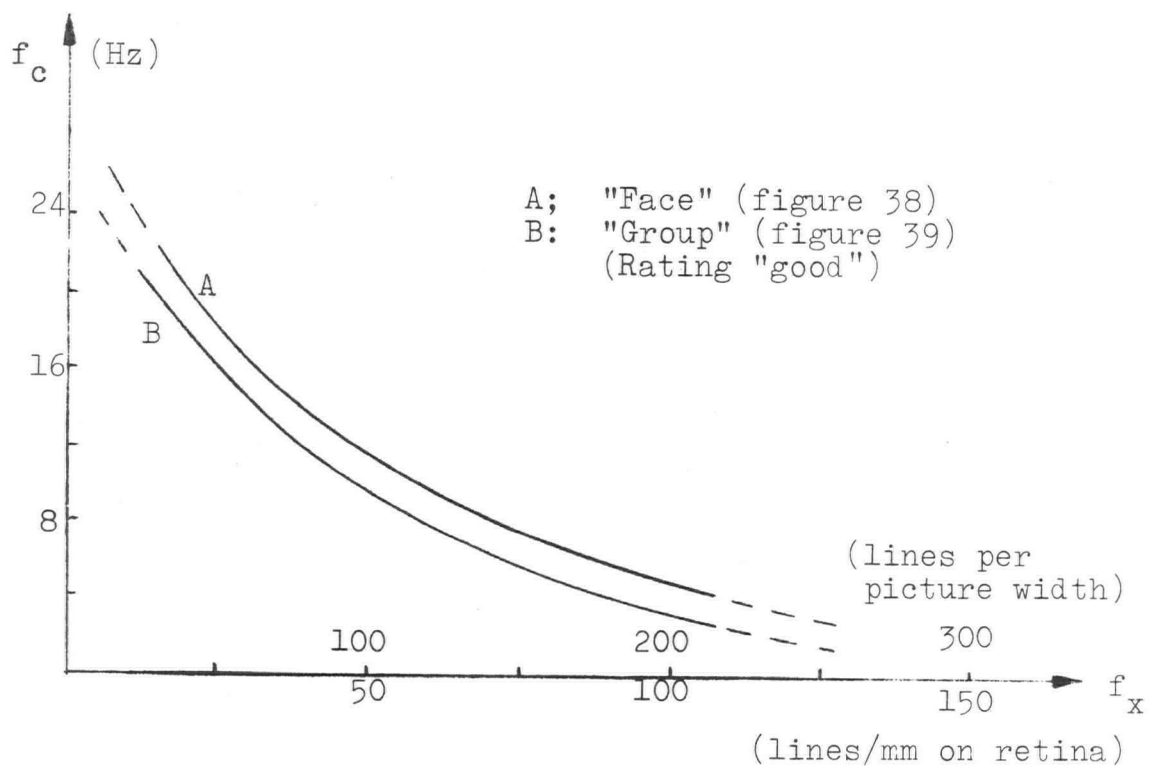


Fig. 40 Critical flicker frequency of two half tone pictures

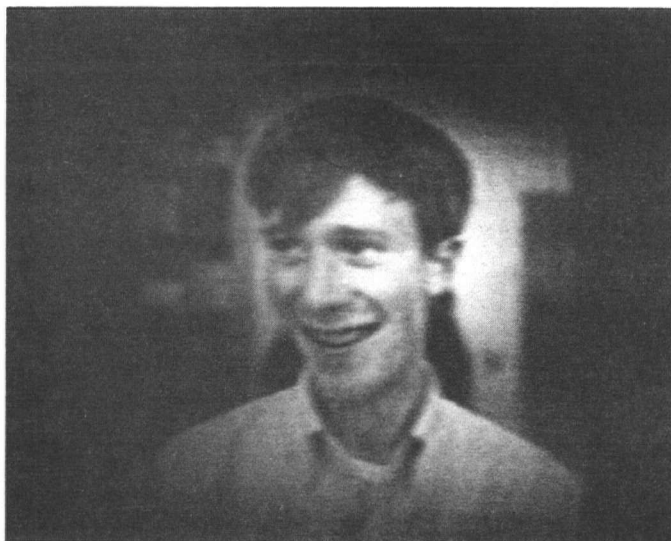


Fig. 41 Bandlimited picture (Resolution 50 lines per picture width)

#### 5.4 A tentative law

One may try to approximate the results shown in the Figures 34, 35, and 40 by a mathematical expression in order to put them into the form of a basic law. It seems that some kind of an exponential function would describe the behaviour of these curves quite well. We may therefore try an expression of the form of equation 5.1

$$f_c = f_0 \exp(-kf_x) \quad 5.1$$

$f_c$  denotes the critical flicker frequency,  $f_x$  the spatial frequency in lines per millimeter on the retina.  $f_0$  is an extrapolated, merely theoretical value for  $f_c$  at a spatial frequency equal to zero. It is not of much practical significance, because for very low spatial frequencies we approach the case of normal "total area" flicker, and judgements of quality are also very difficult to make in this region. The influence of some parameters changes as well, the contrast ratio for example becomes a measure for the average brightness too.

It can be seen, from extrapolation of our curves, that  $f_0$  will depend on the contrast ratio and naturally on the kind of judgement we are working with ("good", "acceptable"). The factor  $k$  in the exponent will also be a parameter depending on the experiment. It is, for example, apparent that  $k$  will be different for the line pattern experiments and for the picture experiments, and it may also depend on the contrast ratio.

The actual experimental values for  $f_0$  generally lie between 24 and 34 Hz. The factor  $k$  lies quite constantly around

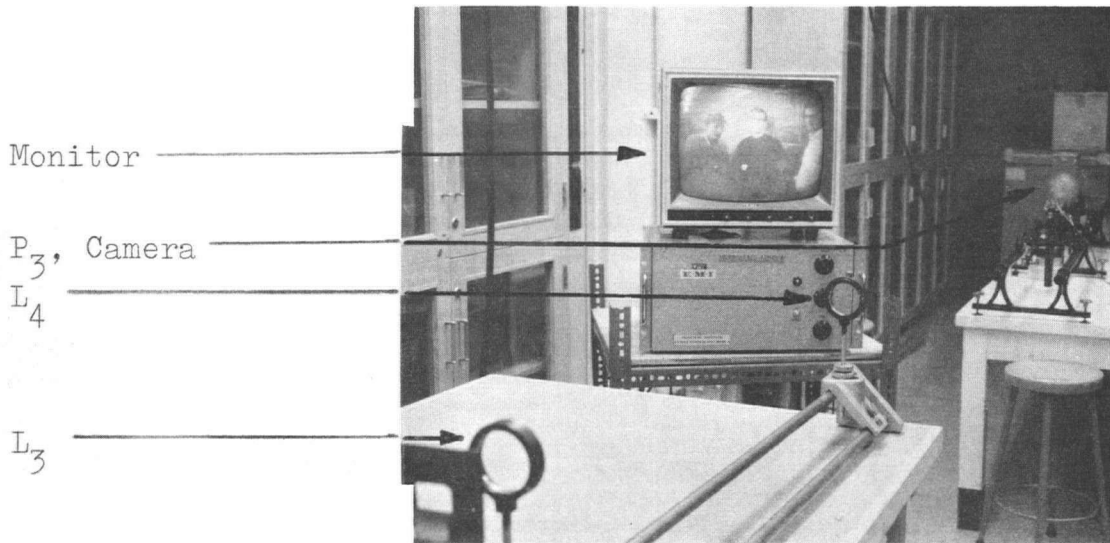
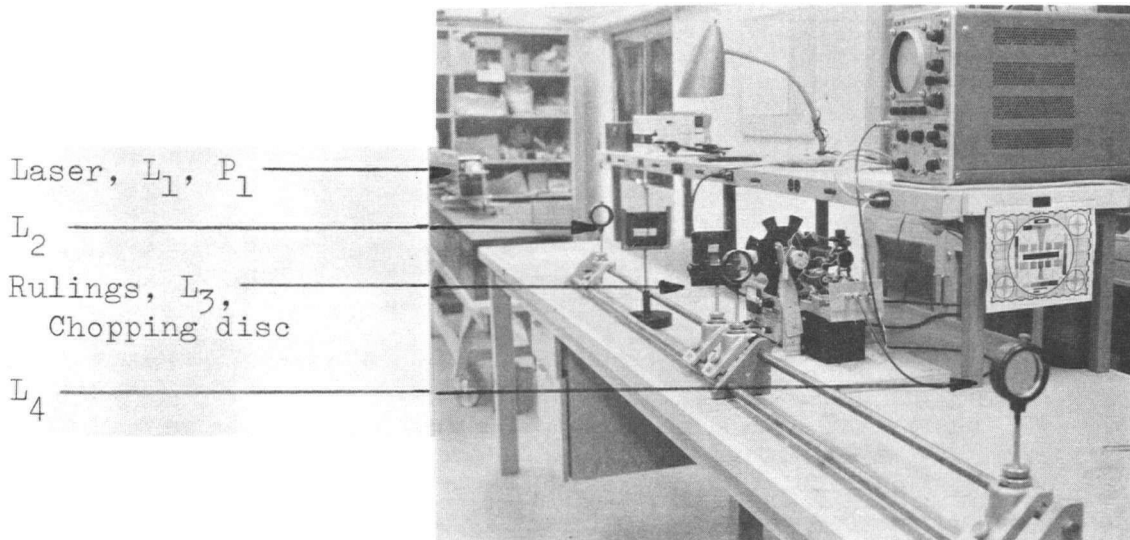
0.012 for all line pattern experiments, and at 0.02 for the pictures.  $k$  generally seems to increase very slightly for increasing contrast ratio.

For curve A of Figure 35 we get the mathematical expression of equation 5.2

$$f_c = 30 \exp(-0.012 f_x) \quad 5.2$$

Curve B of Figure 40 obeys a law according to equation 5.3

$$f_c = 28 \exp(-0.02 f_x) \quad 5.3$$



Figs. 42 and 43 View of test apparatus used  
for the present work

## 6. CONCLUSIONS AND FUTURE WORK

An optical signal processing system may be used conveniently for investigations in the spatial frequency domain of an image signal. This has been the object of the present work, with special emphasis on image compression research. It is not possible at the present time to incorporate an optical system directly in a bandwidth compression scheme; but the results of optical signal processing research can be very useful for study and design of new compression methods.

Some straightforward possibilities of bandwidth compression are apparent for certain test charts which contain very definite spatial frequencies; the large empty regions in their spectra can be omitted to achieve substantial savings in bandwidth. The coarse filtering experiment in chapter 4 showed quite good picture quality for compression ratios ranging from 2 : 1 to 8 : 1 depending on the picture complexity.

The spectra of continuous tone pictures could not be observed accurately enough, because of noise effects; nothing can be said about possibilities of bandwidth compression using spectral gaps for this class of pictures.

Savings in bandwidth can also be achieved by exploiting some characteristics of the human eye. The optical system has been shown to be a very useful tool for investigating one question concerning the visual perception of the eye. The results of these experiments, reported in chapter 5, are very promising with respect to compression possibilities. The decrease in critical flicker frequency for high spatial frequencies of a television picture can be used for compression by presenting the high

spatial frequency content at a reduced rate. Some deterioration of pictures of fast moving scenes will probably occur, similar to the effects reported for a frame repetition and replenishment system<sup>(11)</sup>. Here these effects will be less severe, because the important low frequency content is presented at the normal rate.

The application of optical signal processing to the field of image compression research has produced some interesting results. A number of questions and problems, however, still remain and have to be left for future work. In particular, the following points seem to be of immediate interest:

- a) Additional investigations will have to analyse spectra of "continuous" tone pictures, in which the grey shades are produced by a regularly spaced raster, thus concentrating the spatial frequency content at certain specific points in the spectrum.
- b) Further tests, investigating the critical flicker frequency, have to be carried out, using variable chopping intervals (instead of 50/50 on/off time). A more detailed study of the influence of such parameters as contrast, picture area, brightness, etc. is suggested as well.
- c) There are many ways in which a compression system may be designed using variable presentation rate for different spatial frequency content of a television display. As a first experiment, a very simple system may be built, using only two different repetition rates: Two scanning spots, at different velocities, would produce two signals; one corresponding to

a 1 MHz bandlimited transmission at normal repetition rate (30 frames per second), and one containing the spatial frequencies from 1 to 5 MHz, but at half the repetition rate. The superposition of the two signals at the receiving end could be achieved optically by a suitable viewing arrangement. The compression ratio would only be 1.67 with this system; higher ratios are obviously possible, using more channels, with more differentiated frame repetition rates. Closer realization of the theoretical limit of approximately 3 to 1 is merely a question of system complexity.

## REFERENCES

1. Pratt, W.K., "A Bibliography on Television Bandwidth Reduction Studies", IEEE Trans. on Inf. Theory, vol. IT-13, 1, January 1967.
2. Schreiber, W. F., "Picture Coding", Proc. IEEE, vol. 55, 3, March 1967.
3. Mertz, P., and Gray, F., "A Theory of Scanning and its Relation to the Characteristics of the Transmitted Signal in Telephotography and Television", BSTJ vol. 13, July 1934.
4. Javid, M., and Brenner, E., "Analysis, Transmission and Filtering of Signals", McGraw Hill 1963.
5. Cutrona, L. J., et al., "Optical Data Processing and Filtering Systems", IRE Trans. on Inf. Theory, vol IT-6, June 1960.
6. Vander Lugt, A., "Signal detection by Complex Spatial Filtering", IEEE Trans. on Inf. Theory, vol. IT-10, 1964.
7. Vander Lugt, A. "Operational Notation for the Analysis And Synthesis of Optical Data Processing Systems", Proc. IEEE, vol. 54, 1, Aug. 1966.
8. Born, M., and Wolf, E., "Principles of Optics", Pergamon Press, 2nd edition, Macmillan N.Y. 1964.
9. Anner, G. E., "Elements of Television Systems", Prentice Hall, N.Y. 1951.
10. Seiler, A. J., "Probability Distribution of Television Frame Differences", Proc. IREE Australia, Nov. 1965.
11. Brainard, R. C., et al., "Subjective Effects of Frame Repetition and Picture Replenishment", BSTJ vol. 46, 1, January 1967.
12. DeMott, D. W., "Direct Measures of Retinal Image", JOSA vol. 49, June 1959.
13. Stulz, K. F., and Zweig, H. J., "Relation between Graininess and Granularity for Black and White Samples with Nonuniform Granularity", JOSA vol. 49 June 1959.
14. Lowry, E. M., and dePalma, J. J., "Sine Wave Response of the Visual System", JOSA vol. 51, 7, July 1961.

15. Budrikis, Z. L., Seyler, A. L., "Detail Perception After Scene Changes in Television Image Presentations", IEEE Trans. on Inf. Theory, vol. IT-11, Jan.1965.
16. Biernson, G., "A Feedback-control Model of Human Vision", Proc. IEEE, vol. 54, 6, June 1966.

## APPENDIX

Fourier transform relation of a coherent optical system

Coherent light can be treated as an electromagnetic wave and described by giving its amplitude and phase as a function of the three space variables.

$$U_{x,y,z} = I(x,y,z)\cos[\omega t + \phi(x,y,z)] \quad \text{A.1}$$

For the field in a plane perpendicular to the z-axis in an optical system, we can write

$$U_o = I(x,y)\cos[\omega t + \phi(x,y)] \quad \text{A.2}$$

As a convention, this may also be written in the form

$$\bar{U}_o = I(x,y)\exp[j\phi(x,y)] \quad \text{A.3}$$

This representation is justified by the time invariance of all the significant features of the optical system, where  $\omega$  (the temporal radian frequency of the light) acts in a sense like a carrier frequency.

Let us now consider Figure 2 again (from chapter 2.1), which is repeated here for convenience.

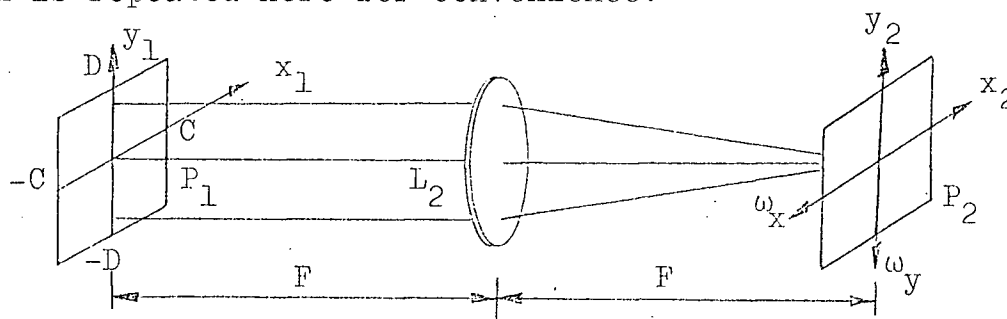


Fig. A.1 Two-dimensional Fourier transformer

In plane  $P_1$  a transparency of the complex transmission function  $\bar{S}(x,y)$  is introduced in the beam of coherent monochromatic light.

$$\bar{S}(x,y) = t(x,y)\exp[j\alpha(x,y)] \quad \text{A.4}$$

Emerging from  $P_1$  is then the multiplication of the light wave with  $\bar{S}(x,y)$

$$\bar{U}_1 = \bar{S} \bar{U}_0 \quad \text{A.5}$$

This wave now is summed up over  $P_1$  onto  $P_2$  by focussing lens  $L_2$ . Calculation of  $\bar{U}_2$  requires finding the optical path length from  $x_1, y_1$  to  $x_2, y_2$ .  $\bar{U}_2$  then is the integral over  $P_1$  of  $\bar{U}_1$ , properly delayed in phase according to the distance  $r$ .

$$\bar{U}_2 = \frac{1}{j\lambda} \iint_{P_1} \frac{1 + \cos\theta}{2d} \bar{U}_1(x,y) \exp\left[-j\frac{2\pi r}{\lambda}\right] dx_1 dy_1 \quad \text{A.6}$$

$\lambda$  = wavelength of light

$d$  = amplitude attenuation factor resulting from distance between  $P_1$  and  $P_2$ .

$\frac{1 + \cos\theta}{2}$  = obliquity factor

$r$  = distance between  $x_1, y_1$  to  $x_2, y_2$ .

In our system,  $\frac{1}{2\lambda}$  can be dropped because absolute phase and amplitude are of no interest,  $d$  is dropped because the attenuation is negligible, and the obliquity factor is dropped because  $\theta$  is always sufficiently small, so that  $\cos\theta \approx 1$ . We then get

$$\bar{U}_2 = \iint_{P_1} \bar{U}_1 \exp \left[ -j \frac{2\pi}{\lambda} r(x_1, y_1, x_2, y_2) \right] dx_1 dy_1 \quad A.7$$

To calculate the distance  $r$ , consider Figure A.2

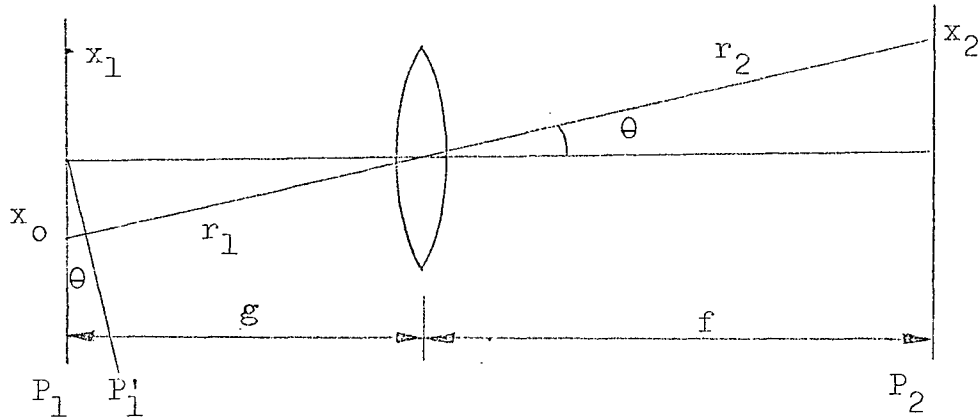


Fig. A.2 Geometrical relations

A plane wave emerging from plane  $P'_1$  at an angle  $\theta$  to the optical axis is brought to focus at  $x_2$ , where  $x_2 = f \sin\theta$ . This implies that the optical distance between  $x_2$  and any point on  $P'_1$  is a constant  $c$ .

$$c = r_1 + r_2 = \sqrt{g^2 - x_0^2 \cos^2 \theta} + \sqrt{f^2 + x_2^2} \quad A.8$$

$$c = g + f + \left(1 + \frac{g}{f}\right) \frac{x_2^2}{2f} \quad \text{for small } \theta \text{ and} \quad A.9$$

taking  $\frac{x_0}{g} = \frac{x_2}{f}$

The distance from the plane  $P'_1$  to  $x_2$  is obtained by adding the term

$$-x_1 \sin\theta = \frac{x_1 x_2}{f} \quad A.10$$

The total distance from  $x_1$  to  $x_2$  is then

$$r(x_1, x_2) = g + f + \left(1 - \frac{g}{f}\right) \frac{x_2^2}{2f} - \frac{x_1 x_2}{f} \quad \text{A.11}$$

In two dimensions, the same approach leads to

$$r(x_1, y_1, x_2, y_2) = \text{const.} \left(1 - \frac{g}{f}\right) \frac{x_2^2 + y_2^2}{2f} - \frac{x_1 x_2}{f} - \frac{y_1 y_2}{f} \quad \text{A.12}$$

For the wave  $\bar{U}_2$  at  $P_2$  we then get

$$\bar{U}_2 = \left[ \iint_{P_1} \bar{U}_1 \exp(-j x x_1) \exp(-j y y_1) dx_1 dy_1 \right] \exp j\beta(\omega_x, \omega_y) \quad \text{A.13}$$

where

$$\omega_x = -\frac{2\pi x_2}{\lambda f} ; \quad \omega_y = -\frac{2\pi y_2}{\lambda f} \quad \text{A.14}$$

and

$$\beta = \left(1 - \frac{g}{f}\right) \frac{x_2^2 + y_2^2}{2f} \quad \text{A.15}$$

For the system of Figure A.1  $g$  is equal to  $f$ , so that  $\beta = 0$ . Equation 2.4 in chapter 2.1 follows immediately. The condition  $f = g$  is necessary to obtain an exact Fourier transform between  $P_1$  and  $P_2$  in this system.